

Title: Slightly nonminimal Hidden sector, Slightly nonthermal relic abundance, and Indirect Detection

Date: Jun 12, 2009 02:50 PM

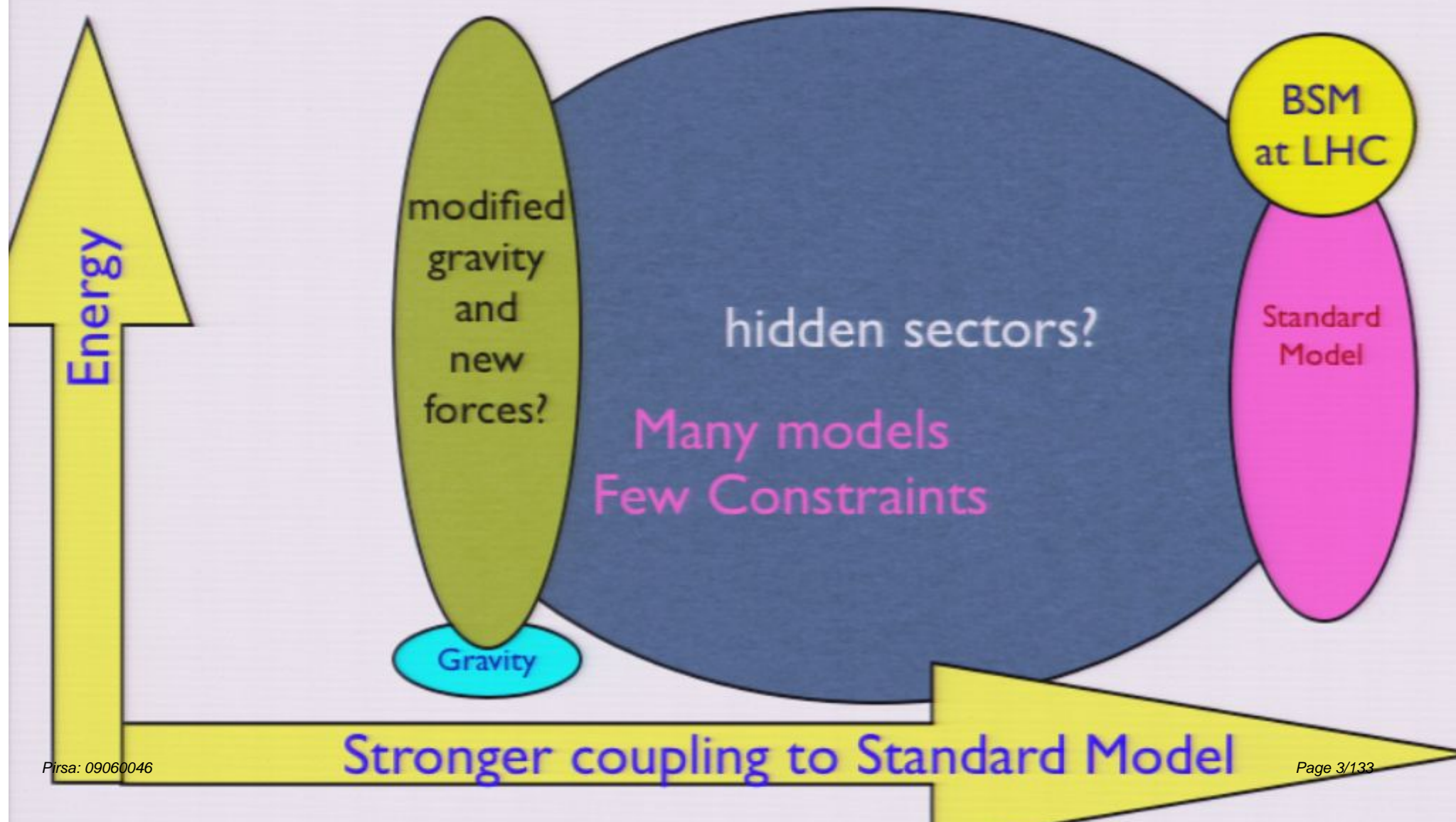
URL: <http://pirsa.org/09060046>

Abstract: I consider a the dark matter relic abundance computation in a model where the dark matter annihilates into a light mediator rather than directly into the standard model. Obtaining the correct relic abundance in such a model may imply a different annihilation cross section than is implied by the usual WIMP decoupling computation. I show that the maximum annihilation cross section is obtained when the hidden sector decouples from the standard model before the dark matter annihilates into the mediator particles, and may be as much as a factor of 5 larger than the standard WIMP value.

Talk Outline

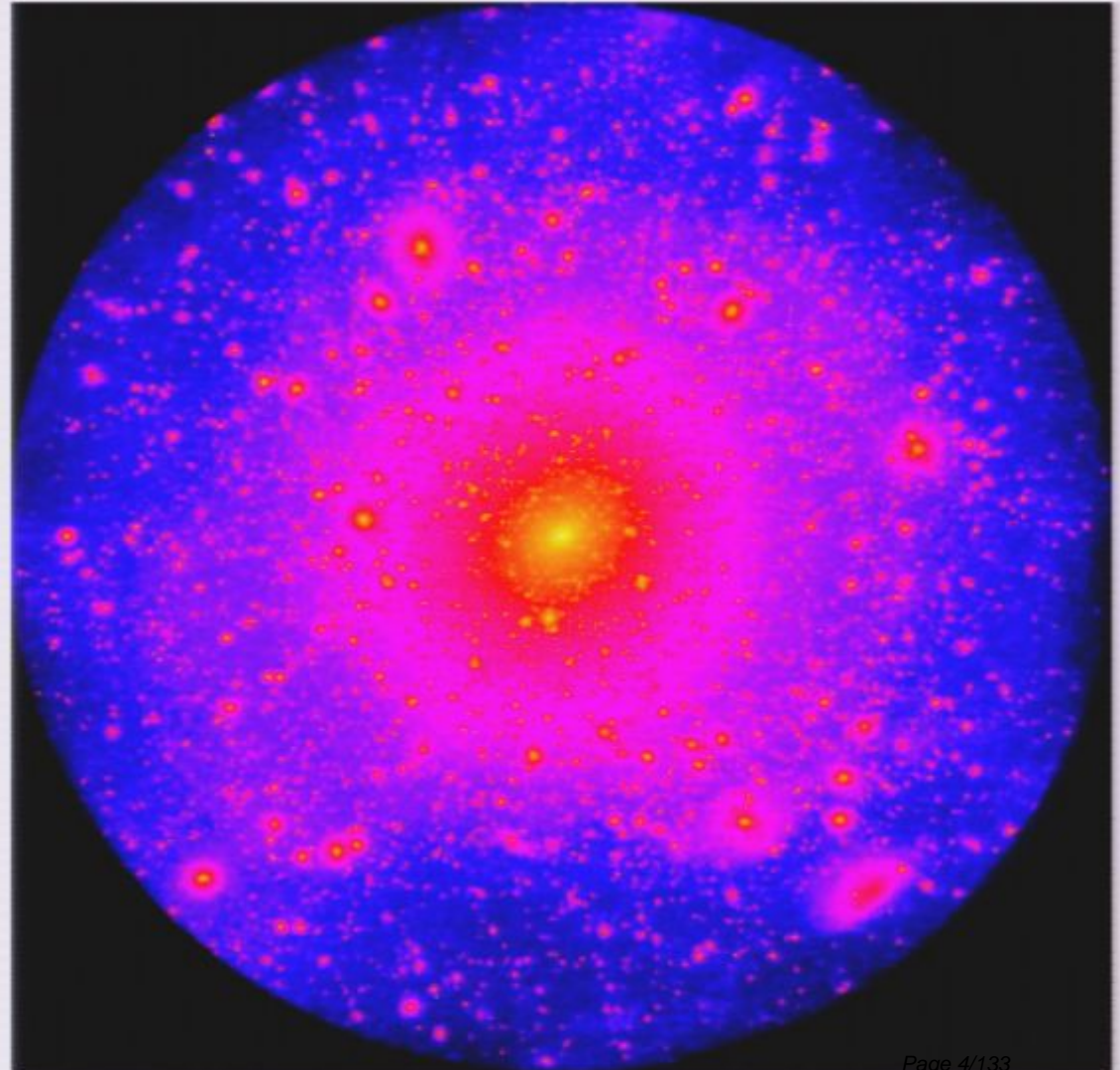
- Quick unnecessary Intro: Indirect detection of dark matter, hidden sectors
- Stripped down hidden sector: slightly nonminimal model of hidden sector dark matter
- Slightly nonthermal relic abundance computation
- Dark Matter annihilation rate
- Comparison with PAMELA, ATIC, Fermi data

Landscape of known and unknown unknowns



Dark Matter Indirect Detection

- Our Dark Galaxy (simulated)
- Very Clumpy, lots of substructure
- annihilation rate/volume $\sim \langle n_x^2 \rangle \sigma v$
- Can we see annihilation products?



Indirect evidence for Dark Matter annihilation seen at Pamela, ATIC, Fermi?

- For ATIC, rate of order 20-1000 x bigger than expected for WIMP (could enhance via clumpiness “boost factor”, Sommerfeld mechanism, and/or have nonthermal production)
- lack of antiprotons a problem for typical WIMPs
- tension with constraints from photons
- Beyond vanilla WIMPS: A new ‘sector’?

Hundreds of new models proposed!



“Slightly nonminimal Dark Matter”

- abstracted and simplified weakly coupled version of hidden sector dark matter, initially inspired to account for PAMELA, ATIC cosmic ray positron and electron excesses
- ‘Slightly nonthermal’ relic abundance computation allows increased cross section for annihilation

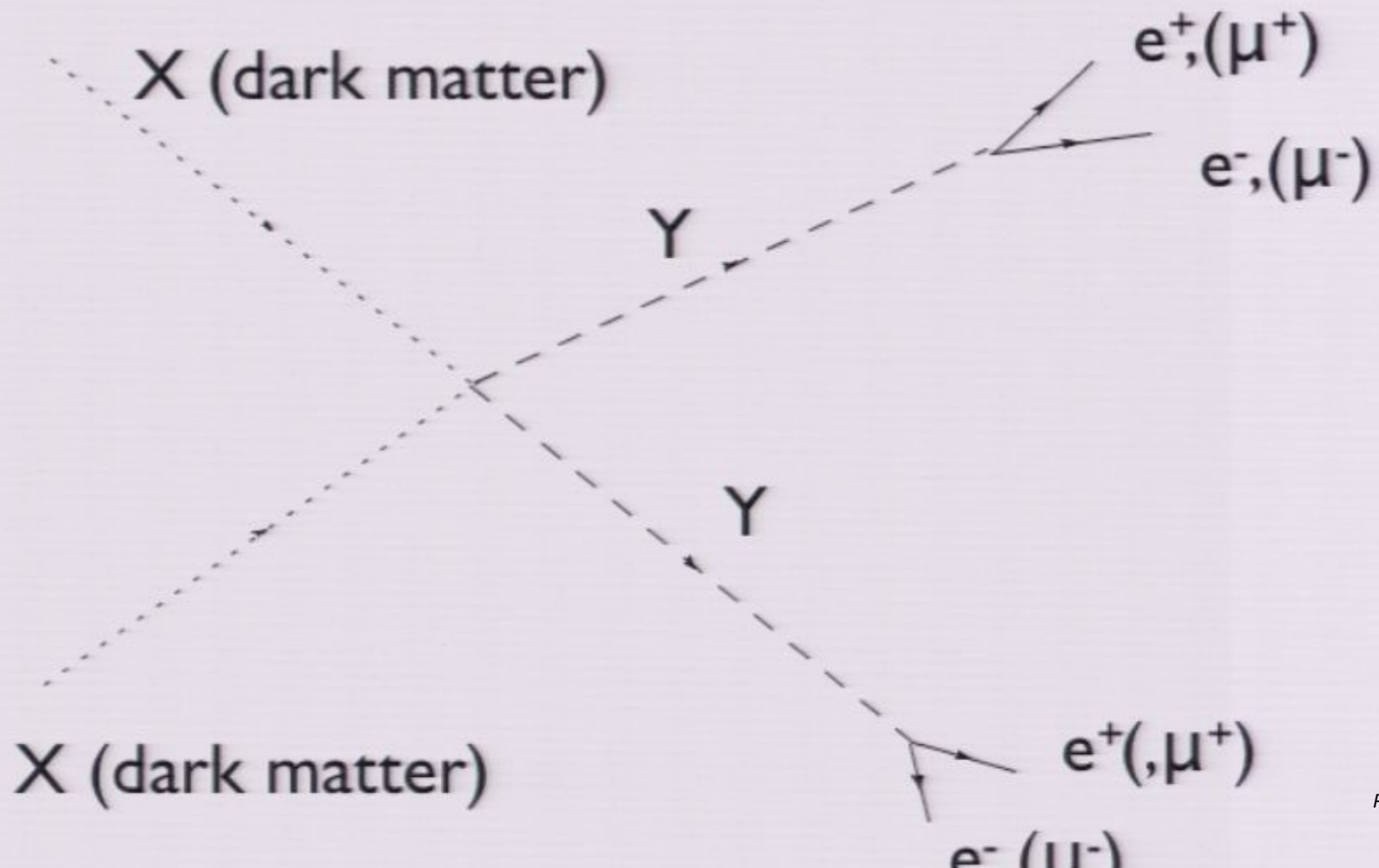
“X-Y-(Z_i) model”

($\bar{\mu}\mu$)

$$\mathcal{L} \supset M^2 X^2 + m^2 Y^2 + \lambda X^2 Y^2 + h Y \bar{e} e$$

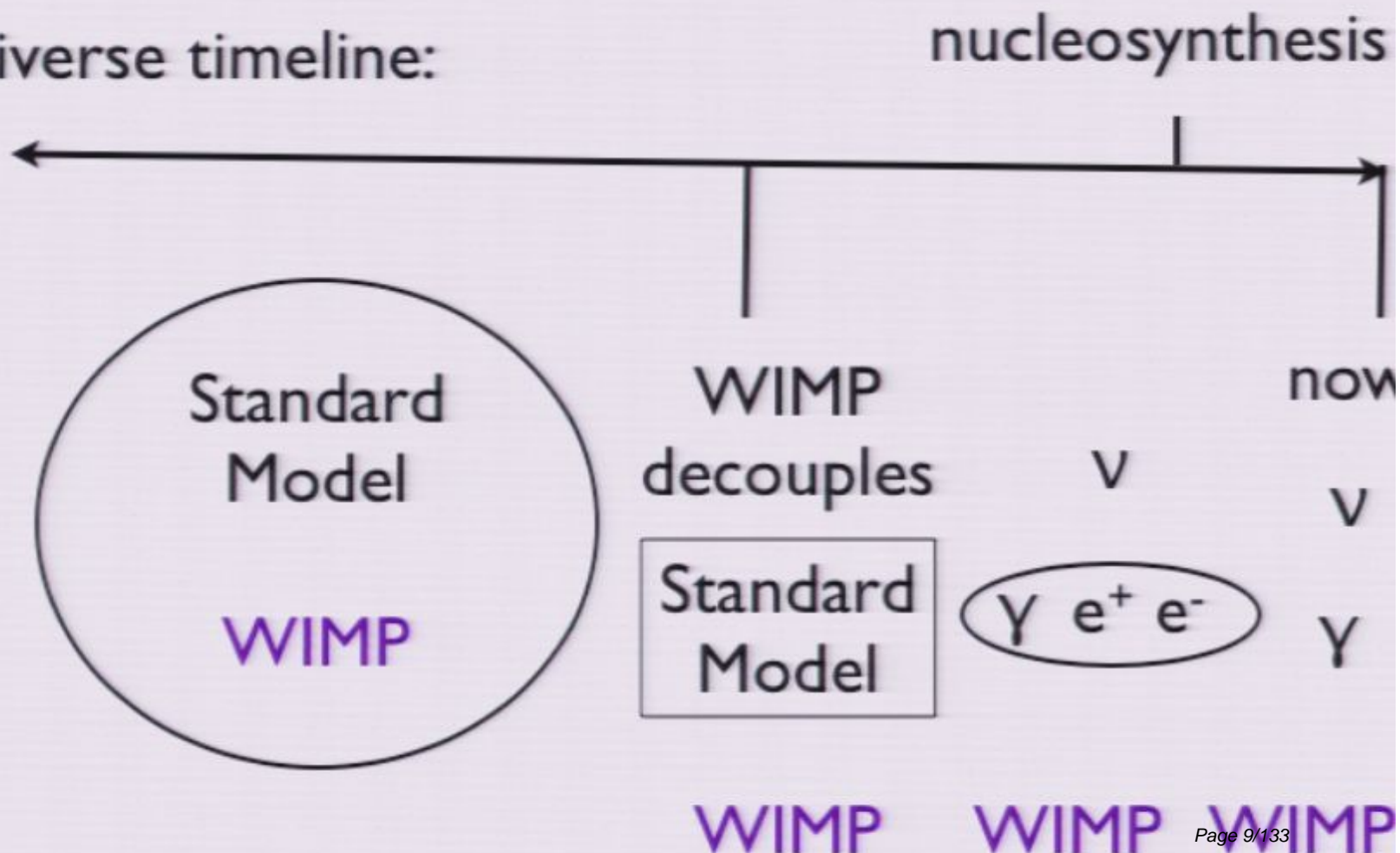
- dark sector contains **at least** 2 new particles
- X, a stable WIMP, no direct SM coupling, mass 20-2000 GeV (scalar or pseudoscalar?)
- Y, a light (~ 100 MeV) metastable ($\tau \sim 0.1$ sec) particle, $\mathcal{O}(1)$ coupling to X, tiny coupling to SM (scalar or pseudoscalar)
- ‘Z_i’, additional, heavier particles
- motivation: “stripped down” exotic strongly coupled dark sector with stable heavy dark matter (X), metastable light bosons (Y), heavier particles (Z_i).

WIMP Annihilation via intermediate light boson



Usual Relic Abundance computation

- Early universe timeline:



Usual Relic Abundance computation

- Rate for annihilations: $\Gamma \approx n_X v \sigma$, where

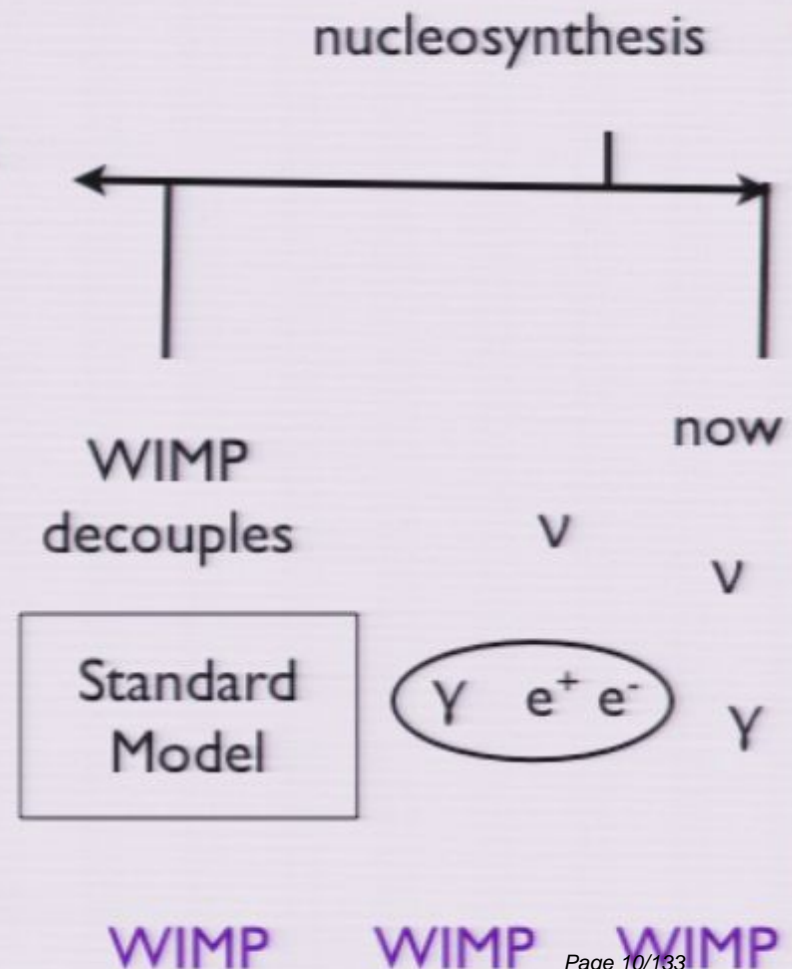
- n_X is WIMP density, v is velocity
- σ is annihilation cross section $\sim 1/v$.
- in equilibrium

$$n_X \sim (M_X T_{\text{hid}})^{3/2} e^{(-M_X/T_{\text{hid}})}$$

- WIMP abundance/comoving volume frozen when $\Gamma \sim 1/t \sim H \sim \rho^{1/2}/m_P$

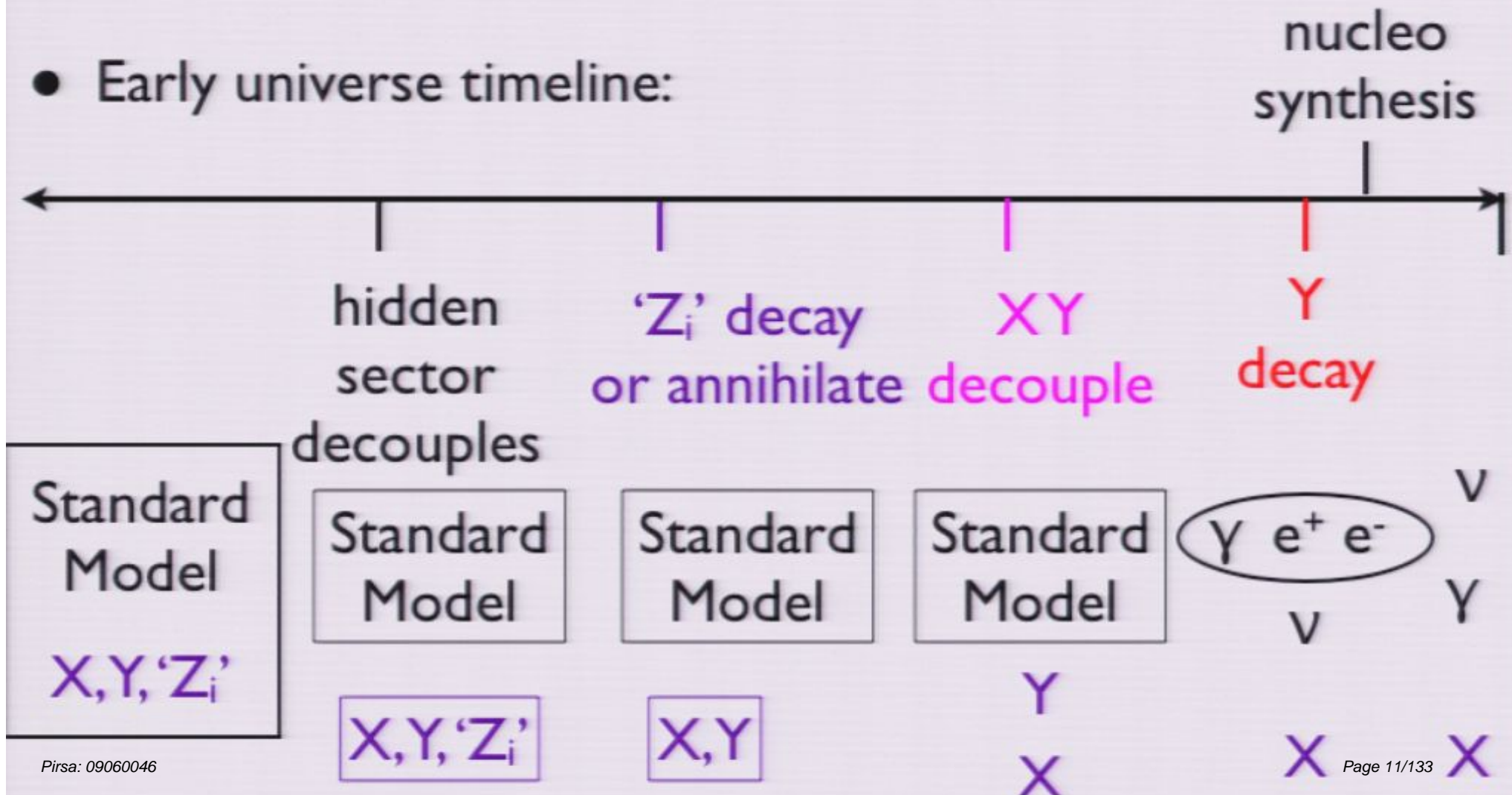
- ρ is energy density

- \sim constant WIMP/entropy ratio after freezeout



Relic Abundance in X-Y- Z_i model

- Early universe timeline:



freezeout and relic X abundance in X-Y(Z) model nucleo synthesis

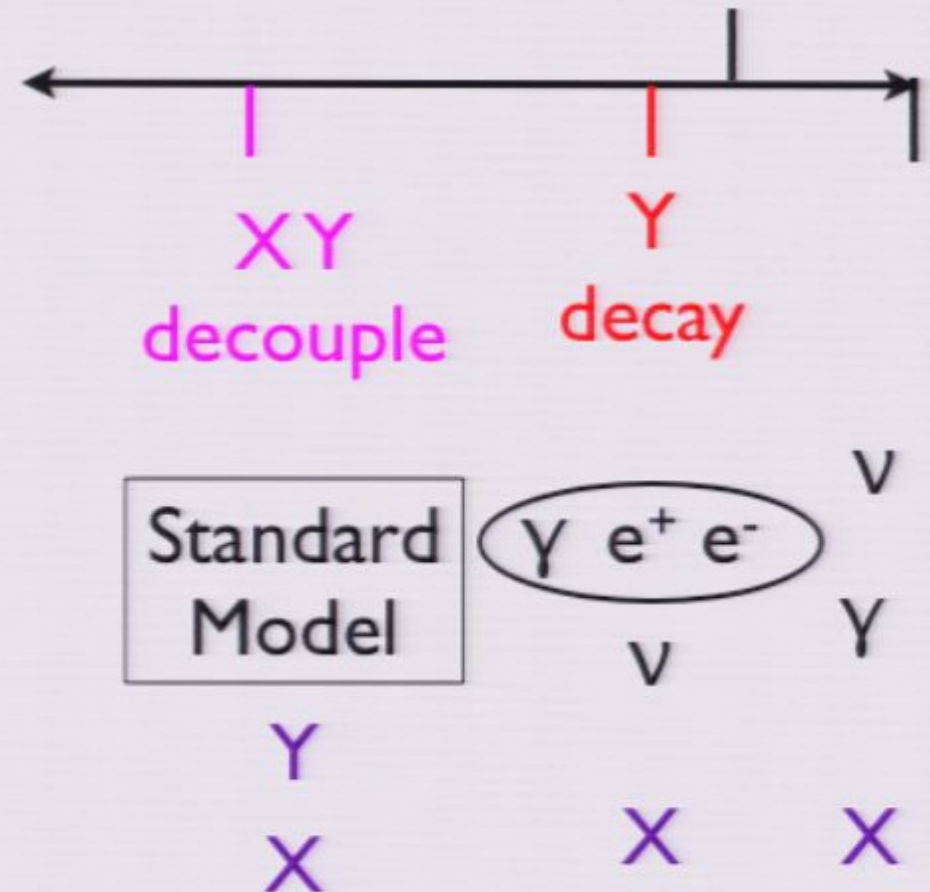
- $T_{\text{vis}} < T_{\text{hid}}$

- $\rho_{\text{hid}} \sim g_{\text{hid}}^* T_{\text{hid}}^4$

- $g_{\text{hid}}^* = 1$ (dominated by Y)

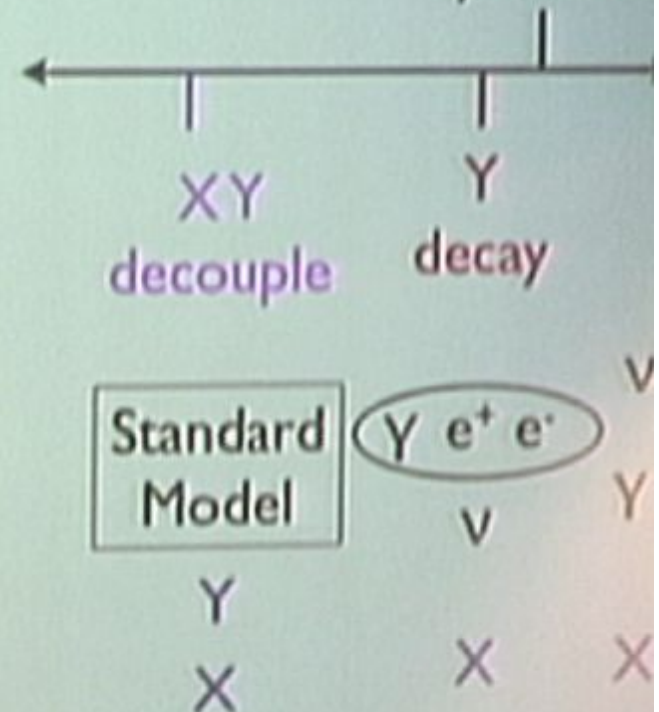
- in early universe energy density $\rho \sim g^* T^4 + T_{\text{hid}}^4$

- $g^* \sim 86.25$ in SM at 30 GeV
(g^* : effective number of degrees of freedom)



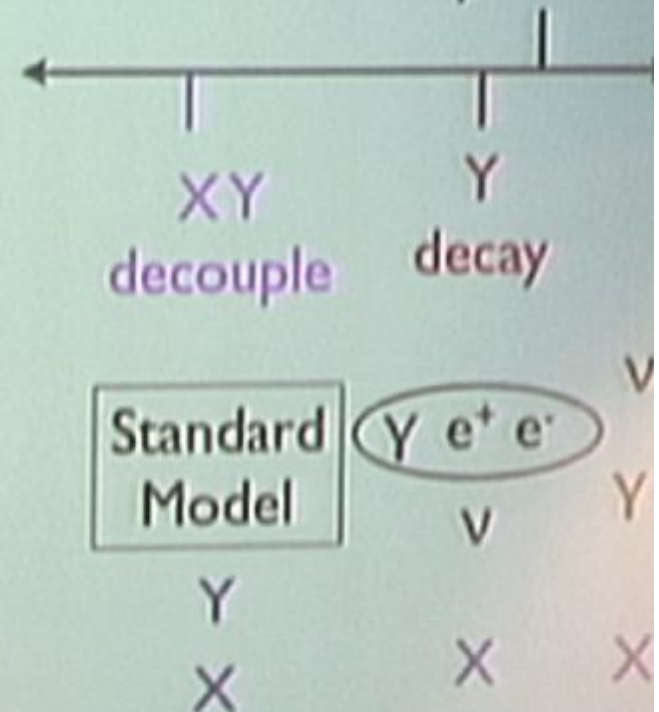
X freezeout and relic X abundance in X-Y(Z) model nucleosynthesis

- $T_{\text{vis}} < T_{\text{hid}}$
- $\rho_{\text{hid}} \sim g_{\text{hid}} T_{\text{hid}}^4$
- $g_{\text{hid}} = 1$ (dominated by Y)
- in early universe energy density $\rho \sim g_* T^4 + T_{\text{hid}}^4$
- $g_* \sim 86.25$ in SM at 30 GeV
(g_* : effective number of degrees of freedom)



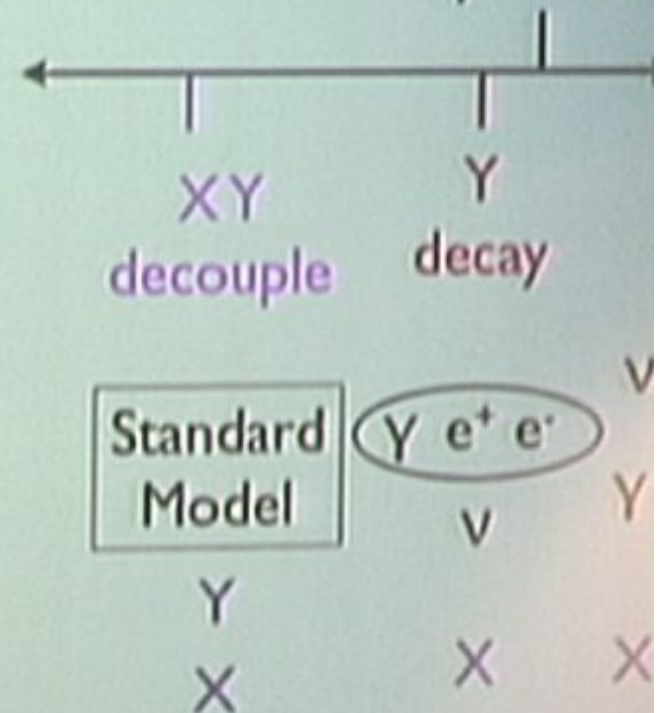
X freezeout and relic X abundance in X-Y(Z) model nucleosynthesis

- $T_{\text{vis}} < T_{\text{hid}}$
- $\rho_{\text{hid}} \sim g_{\text{hid}}^* T_{\text{hid}}^4$
- $g_{\text{hid}}^* = 1$ (dominated by Y)
- in early universe energy density $\rho \sim g_* T^4 + T_{\text{hid}}^4$
- $g_* \sim 86.25$ in SM at 30 GeV
(g_* : effective number of degrees of freedom)



X freezeout and relic X abundance in X-Y(Z) model nucleosynthesis

- $T_{\text{vis}} < T_{\text{hid}}$
- $\rho_{\text{hid}} \sim g_{\text{hid}}^* T_{\text{hid}}^4$
- $g_{\text{hid}}^* = 1$ (dominated by Y)
- in early universe energy density $\rho \sim g_* T^4 + T_{\text{hid}}^4$
- $g_* \sim 86.25$ in SM at 30 GeV (g_* : effective number of degrees of freedom)



freezeout and relic X abundance in X-Y(Z) model nucleo synthesis

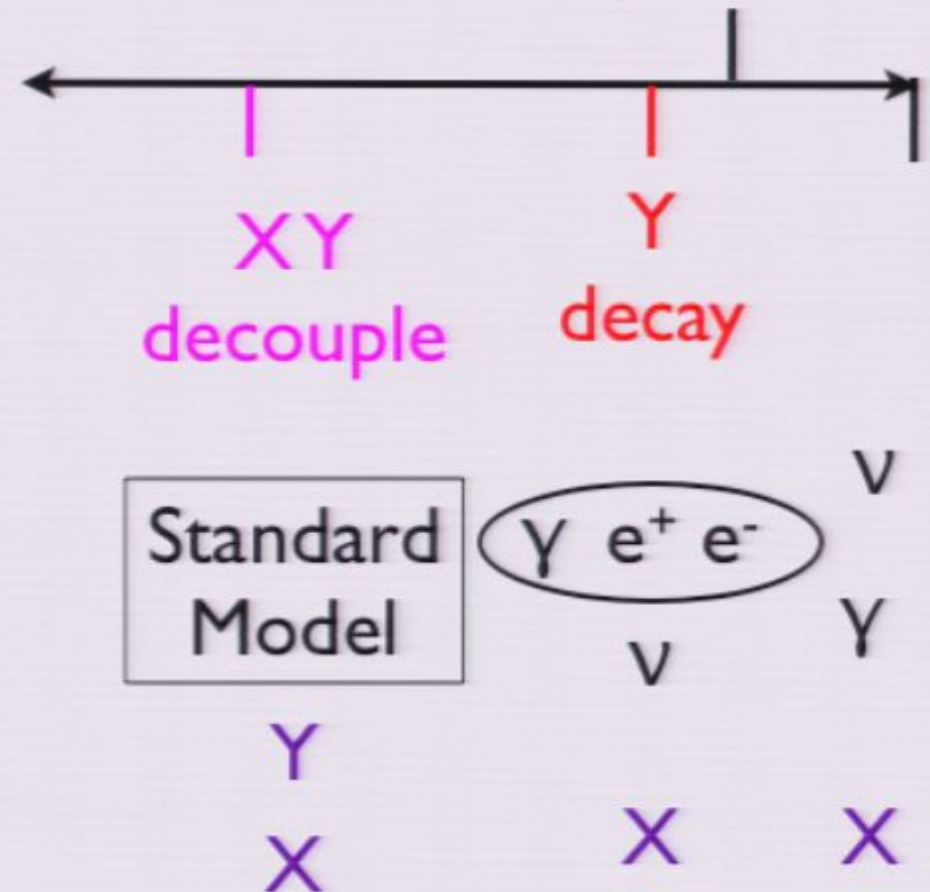
- $T_{\text{vis}} < T_{\text{hid}}$

- $\rho_{\text{hid}} \sim g_{\text{hid}}^* T_{\text{hid}}^4$

- $g_{\text{hid}}^* = 1$ (dominated by Y)

- in early universe energy density $\rho \sim g^* T^4 + T_{\text{hid}}^4$

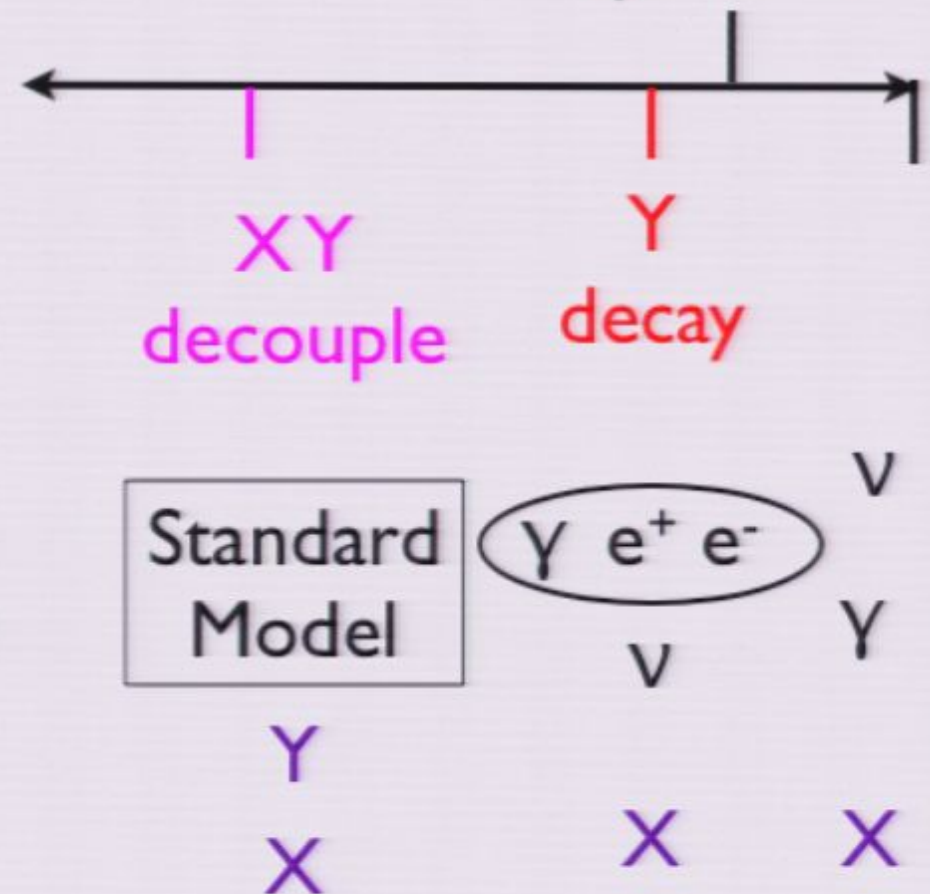
- $g^* \sim 86.25$ in SM at 30 GeV
(g^* : effective number of degrees of freedom)



Freezeout and relic X abundance in X-Y(Z) model

- XY Freezeout:

$$(M T_{\text{hid}})^{3/2} e^{(-M/T_{\text{hid}})} \sigma v \sim (g^* T^4 + T_{\text{hid}}^4)^{1/2} / m_P$$
- WIMP density /entropy ratio n_X/s conserved until Y decay
- entropy $s \sim g^* T^3 + T_{\text{hid}}^3$
- entropy created during Y decay to e^+e^- (or $\mu^+\mu^-$)



X freezeout and relic X abundance in X-Y(Z) model nucleosynthesis

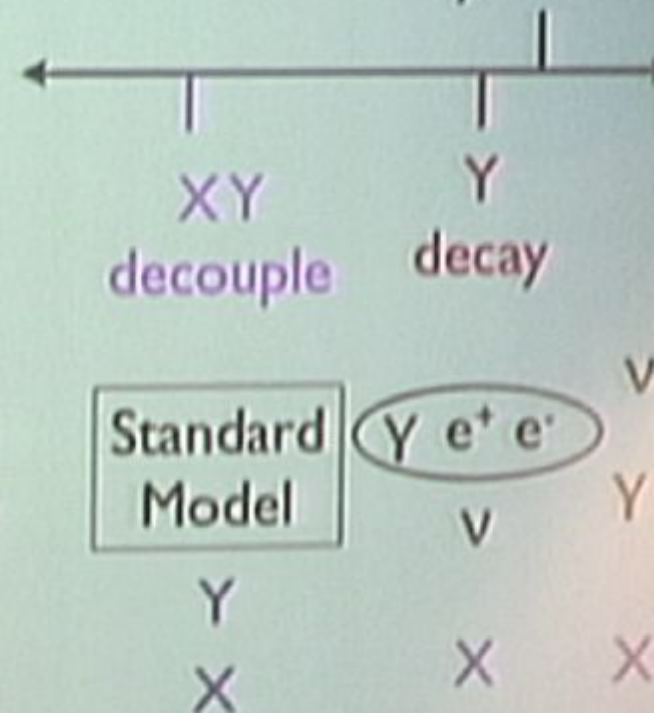
• XY Freezeout:

$$(M T_{\text{hid}})^{3/2} e^{(-M/T_{\text{hid}})} \sigma v \sim (g_* T^4 + T_{\text{hid}}^4)^{1/2} / m_P$$

• WIMP density /entropy ratio n_X/s conserved until Y decay

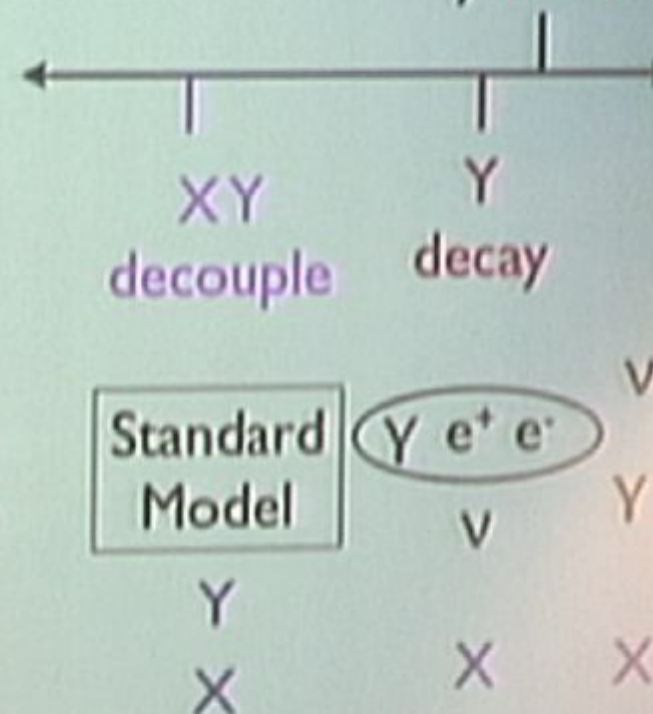
• entropy $s \sim g_* T^3 + T_{\text{hid}}^3$

• entropy created during Y decay to e^+e^- (or $\mu^+\mu^-$)



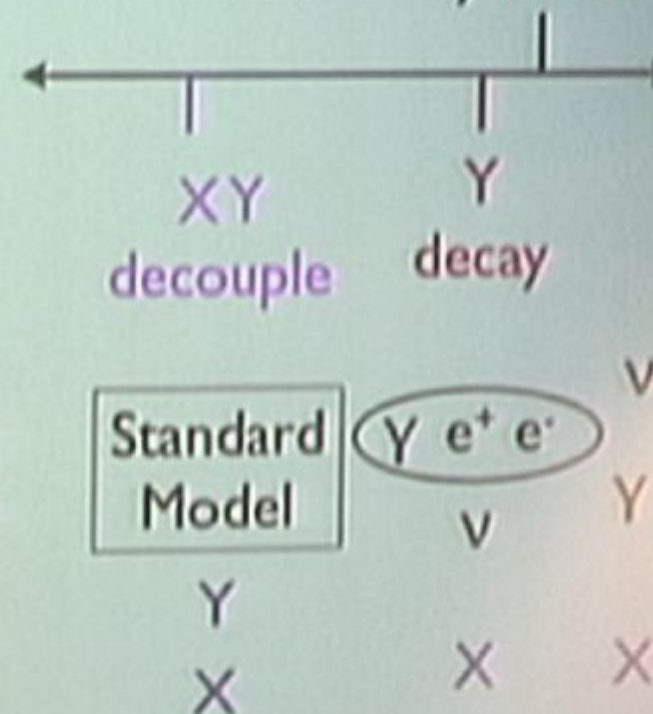
X freezeout and relic X abundance in X-Y(Z) model nucleosynthesis

- XY Freezeout:
 $(M T_{\text{hid}})^{3/2} e^{(-M/T_{\text{hid}})} \sigma v \sim (g_* T^4 + T_{\text{hid}}^4)^{1/2} / m_P$
- WIMP density /entropy ratio n_X/s conserved until Y decay
- entropy $s \sim g_* T^3 + T_{\text{hid}}^3$
- entropy created during Y decay to e^+e^- (or $\mu^+\mu^-$)



X freezeout and relic X abundance in X-Y(Z) model nucleosynthesis

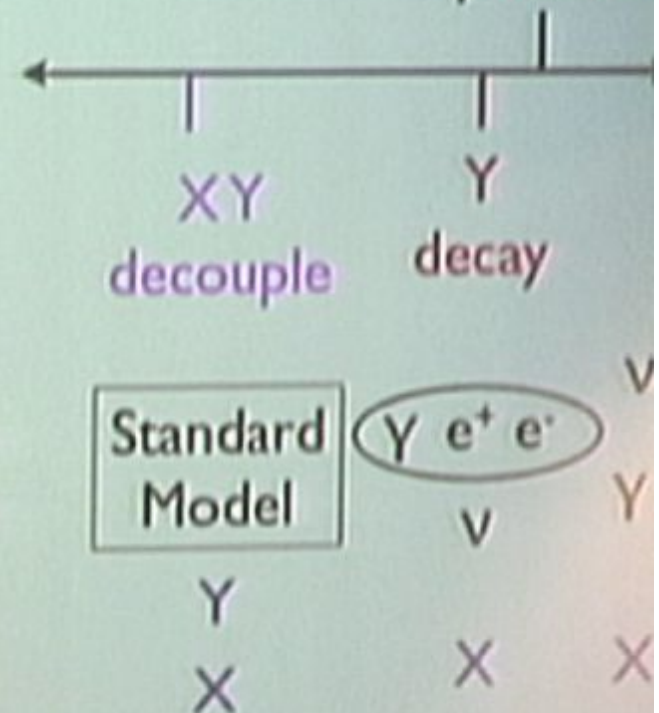
- XY Freezeout:
 $(M T_{\text{hid}})^{3/2} e^{(-M/T_{\text{hid}})} \sigma v \sim (g_* T^4 + T_{\text{hid}}^4)^{1/2} / m_P$
- WIMP density /entropy ratio n_X/s conserved until Y decay
- entropy $s \sim g_* T^3 + T_{\text{hid}}^3$
- entropy created during Y decay to e^+e^- (or $\mu^+\mu^-$)



X freezeout and relic X abundance in X-Y(Z) model nucleosynthesis

- XY Freezeout:

$$(M T_{\text{hid}})^{3/2} e^{(-M/T_{\text{hid}})} \sigma v \sim (g_* T^4 + T_{\text{hid}}^4)^{1/2} / m_P$$
- WIMP density /entropy ratio n_X/s conserved until Y decay
- entropy $s \sim g_* T^3 + T_{\text{hid}}^3$
- entropy created during Y decay to e^+e^- (or $\mu^+\mu^-$)



Freezeout and relic X abundance in X-Y(Z) model

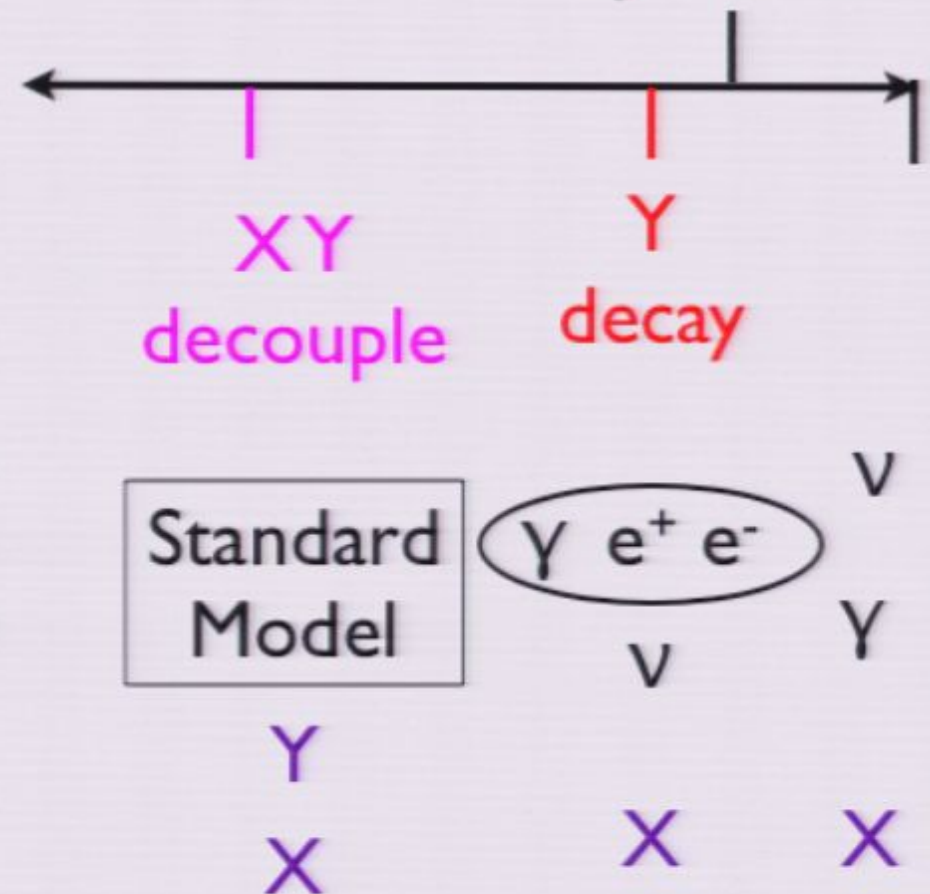
• XY Freezeout:

$$(M T_{\text{hid}})^{3/2} e^{(-M/T_{\text{hid}})} \sigma v \sim (g^* T^4 + T_{\text{hid}}^4)^{1/2} / m_P$$

• WIMP density /entropy ratio n_X/s conserved until Y decay

• entropy $s \sim g^* T^3 + T_{\text{hid}}^3$

• entropy created during Y decay to e^+e^- (or $\mu^+\mu^-$)



X freezeout and relic X abundance in X-Y(Z) model nucleosynthesis

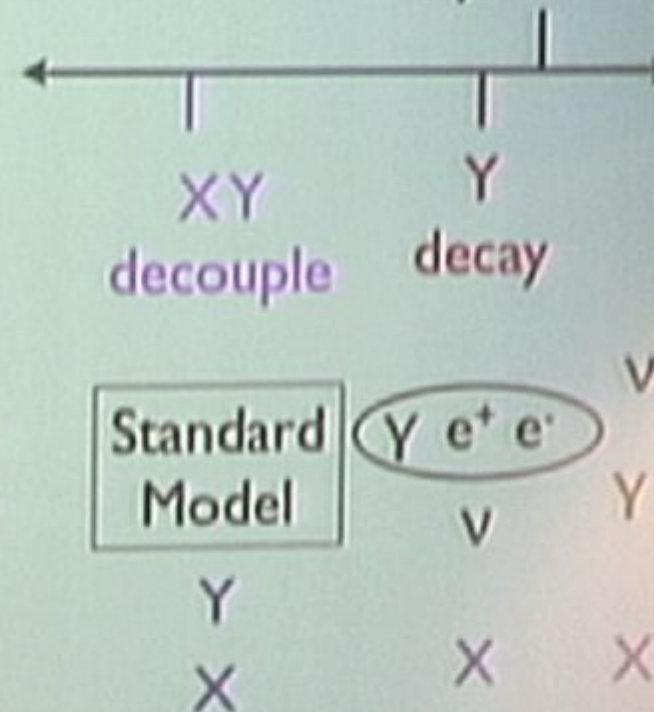
• XY Freezeout:

$$(M T_{\text{hid}})^{3/2} e^{(-M/T_{\text{hid}})} \sigma v \sim (g_* T^4 + T_{\text{hid}}^4)^{1/2} / m_P$$

• WIMP density /entropy ratio n_i/s conserved until Y decay

• entropy $s \sim g_* T^3 + T_{\text{hid}}^3$

• entropy created during Y decay to e^+e^- (or $\mu^+\mu^-$)



X freezeout and relic X abundance in X-Y(Z) model nucleosynthesis

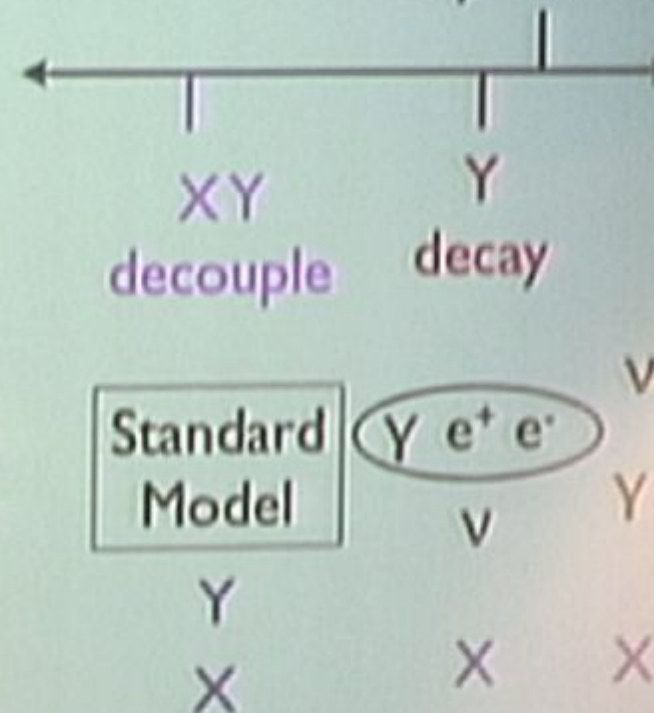
• XY Freezeout:

$$(M T_{\text{hid}})^{3/2} e^{(-M/T_{\text{hid}})} \sigma v \sim (g_* T^4 + T_{\text{hid}}^4)^{1/2} / m_P$$

• WIMP density/entropy ratio n_X/s conserved until Y decay

• entropy $s \sim g_* T^3 + T_{\text{hid}}^3$

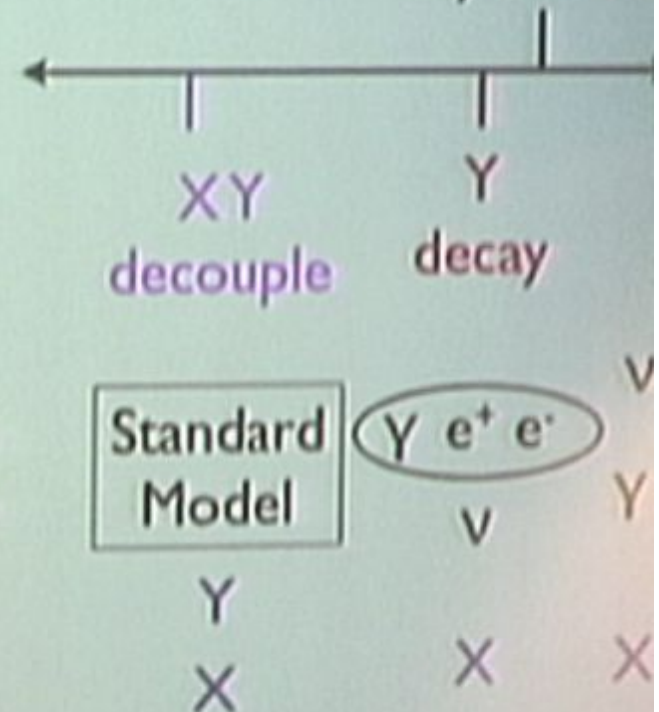
• entropy created during Y decay to e^+e^- (or $\mu^+\mu^-$)



X freezeout and relic X abundance in X-Y(Z) model nucleosynthesis

- XY Freezeout:

$$(M T_{\text{hid}})^{3/2} e^{(-M/T_{\text{hid}})} \sigma v \sim (g_* T^4 + T_{\text{hid}}^4)^{1/2} / m_P$$
- WIMP density /entropy ratio n_X/s conserved until Y decay
- entropy $s \sim g_* T^3 + T_{\text{hid}}^3$
- entropy created during Y decay to e^+e^- (or $\mu^+\mu^-$)



X freezeout and relic X abundance in X-Y(Z) model nucleosynthesis

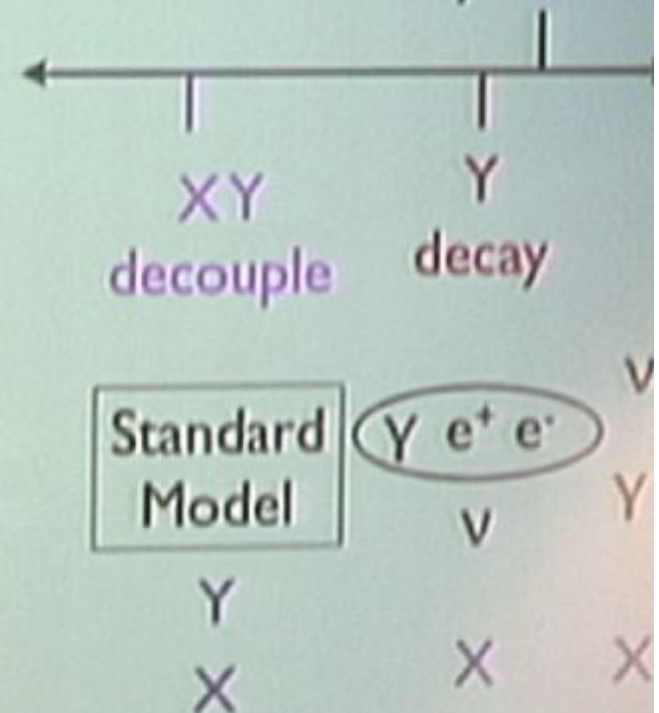
• XY Freezeout:

$$(M T_{\text{hid}})^{3/2} e^{(-M/T_{\text{hid}})} \sigma v \sim (g_* T^4 + T_{\text{hid}}^4)^{1/2} / m_P$$

• WIMP density /entropy ratios conserved until Y decay

• entropy $s \sim g_* T^3 + T_{\text{hid}}^3$

• entropy created during Y decay to e^+e^- (or $\mu^+\mu^-$)



X freezeout and relic X abundance in X-Y(Z) model nucleosynthesis

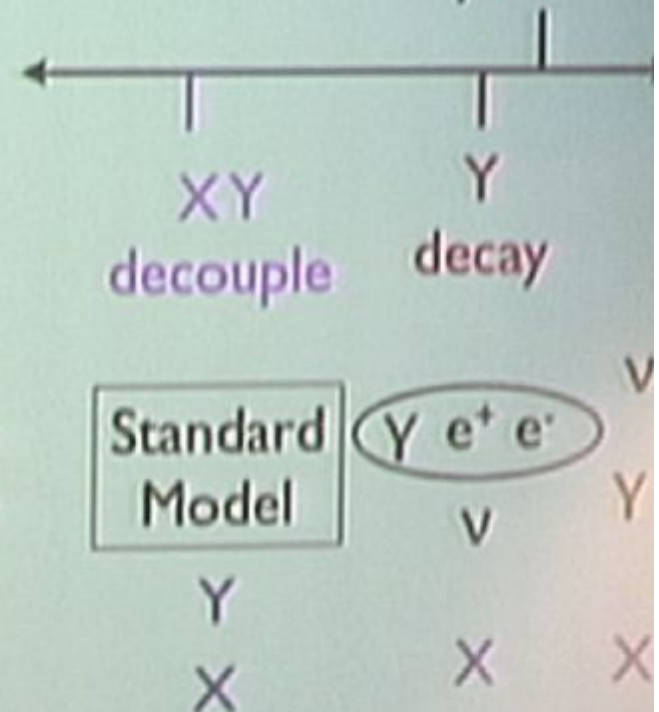
• XY Freezeout:

$$(M T_{\text{hid}})^{3/2} e^{(-M/T_{\text{hid}})} \sigma v \sim (g_* T^4 + T_{\text{hid}}^4)^{1/2} / m_P$$

• WIMP density / entropy ratio n_X/s conserved until Y decay

• entropy $s \sim g_* T^3 + T_{\text{hid}}^3$

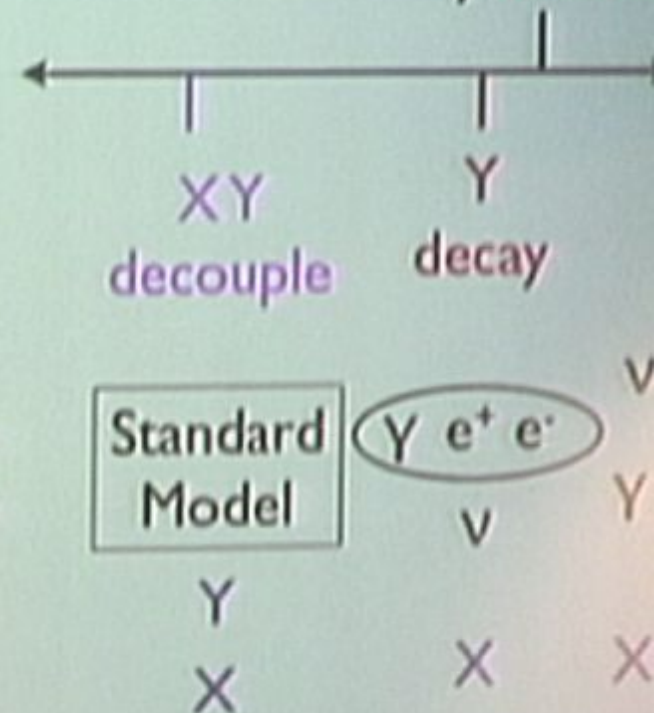
• entropy created during Y decay to e^+e^- (or $\mu^+\mu^-$)



X freezeout and relic X abundance in X-Y(Z) model nucleosynthesis

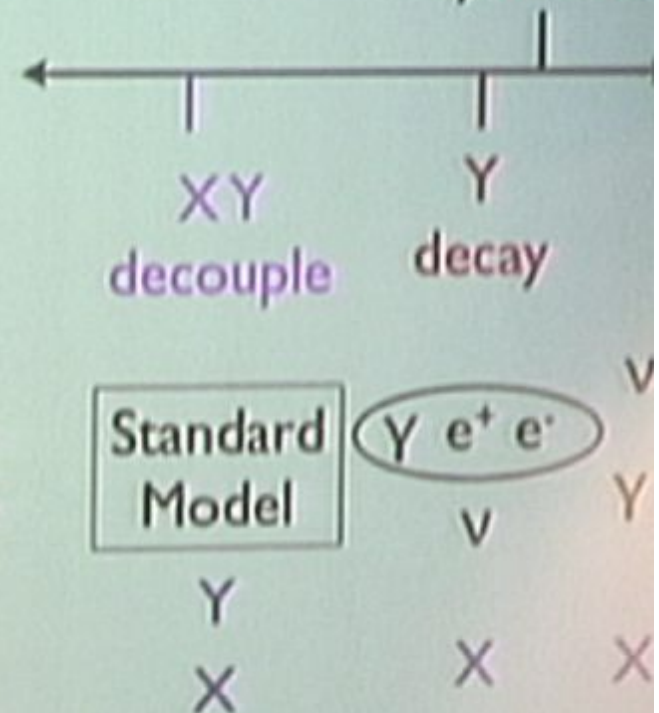
- XY Freezeout:

$$(M T_{\text{hid}})^{3/2} e^{(-M/T_{\text{hid}})} \sigma v \sim (g_* T^4 + T_{\text{hid}}^4)^{1/2} / m_P$$
- WIMP density /entropy ratio n_X/s conserved until Y decay
- entropy $s \sim g_* T^3 + T_{\text{hid}}^3$
- entropy created during Y decay to e^+e^- (or $\mu^+\mu^-$)



X freezeout and relic X abundance in X-Y(Z) model nucleosynthesis

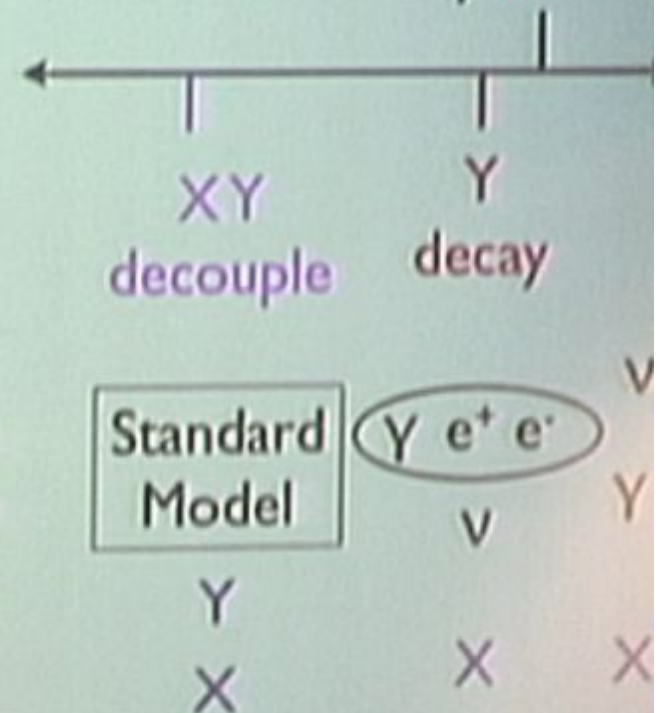
- XY Freezeout:
 $(M T_{\text{hid}})^{3/2} e^{(-M/T_{\text{hid}})} \sigma v \sim (g_* T^4 + T_{\text{hid}}^4)^{1/2} / m_P$
- WIMP density /entropy ratio n_X/s conserved until Y decay
- entropy $s \sim g_* T^3 + T_{\text{hid}}^3$
- entropy created during Y decay to e^+e^- (or $\mu^+\mu^-$)



X freezeout and relic X abundance in X-Y(Z) model nucleosynthesis

- XY Freezeout:

$$(M T_{\text{hid}})^{3/2} e^{(-M/T_{\text{hid}})} \sigma v \sim (g_* T^4 + T_{\text{hid}}^4)^{1/2} / m_P$$
- WIMP density /entropy ratio n_X/s conserved until Y decay
- entropy $s \sim g_* T^3 + T_{\text{hid}}^3$
- entropy created during Y decay to e^+e^- (or $\mu^+\mu^-$)



Freezeout and relic X abundance in X-Y(Z) model

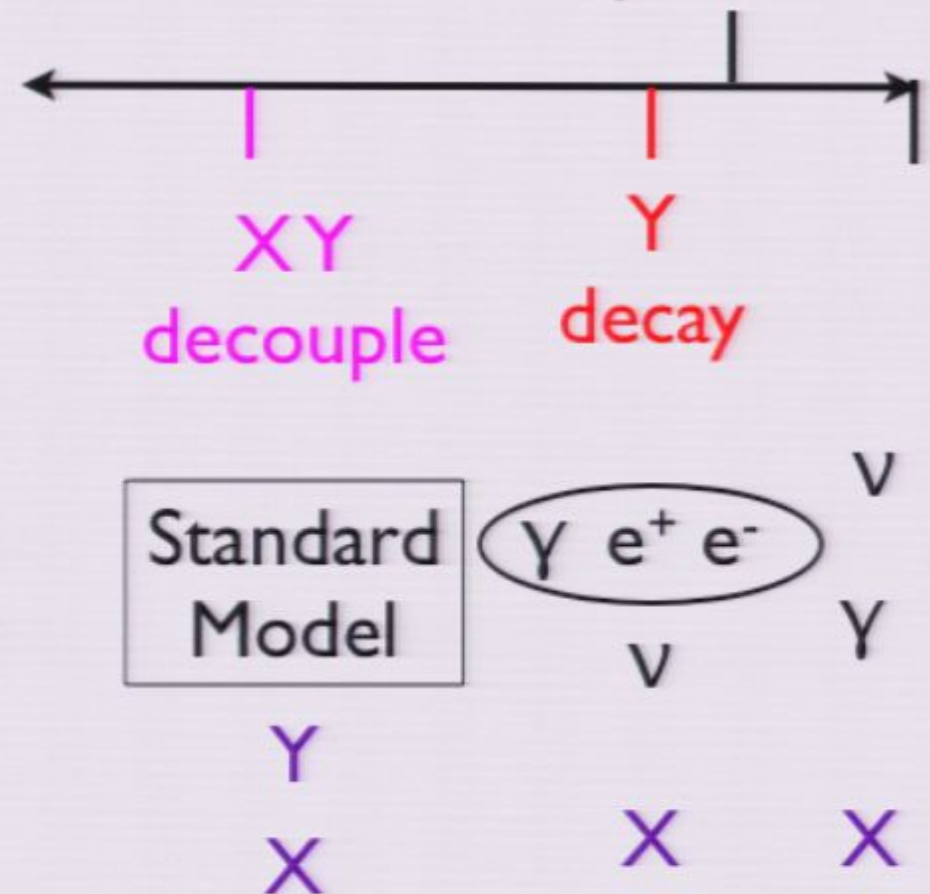
• XY Freezeout:

$$(M T_{\text{hid}})^{3/2} e^{(-M/T_{\text{hid}})} \sigma v \sim (g^* T^4 + T_{\text{hid}}^4)^{1/2} / m_P$$

• WIMP density /entropy ratio n_X/s conserved until Y decay

• entropy $s \sim g^* T^3 + T_{\text{hid}}^3$

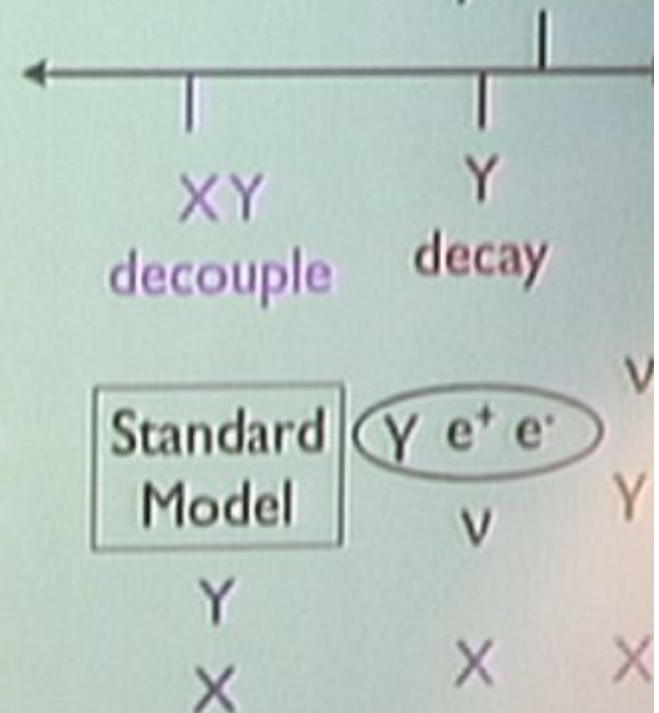
• entropy created during Y decay to e^+e^- (or $\mu^+\mu^-$)



X freezeout and relic X abundance in X-Y(Z) model nucleosynthesis

- XY Freezeout:

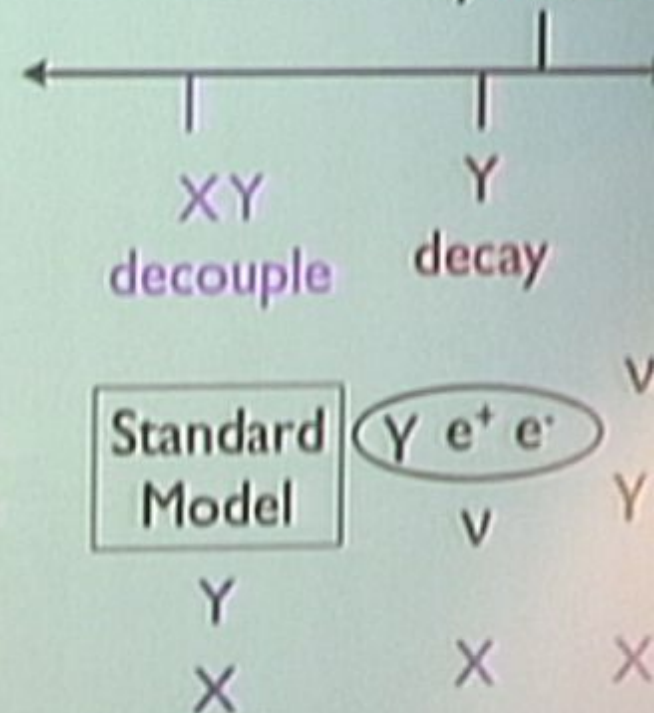
$$(M T_{\text{hid}})^{3/2} e^{(-M/T_{\text{hid}})} \sigma v \sim (g_* T^4 + T_{\text{hid}}^4)^{1/2} / m_P$$
- WIMP density /entropy ratio n/s conserved until Y decay
- entropy $s \sim g_* T^3 + T_{\text{hid}}^3$
- entropy created during Y decay to e^+e^- (or $\mu^+\mu^-$)



X freezeout and relic X abundance in X-Y(Z) model nucleosynthesis

- XY Freezeout:

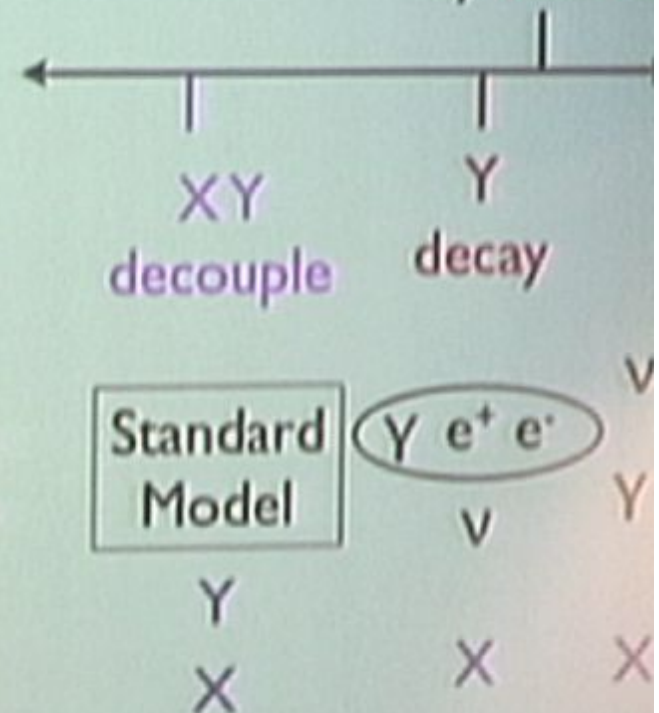
$$(M T_{\text{hid}})^{3/2} e^{(-M/T_{\text{hid}})} \sigma v \sim (g_* T^4 + T_{\text{hid}}^4)^{1/2} / m_P$$
- WIMP density /entropy ratio n_X/s conserved until Y decay
- entropy $s \sim g_* T^3 + T_{\text{hid}}^3$
- entropy created during Y decay to e^+e^- (or $\mu^+\mu^-$)



X freezeout and relic X abundance in X-Y(Z) model nucleosynthesis

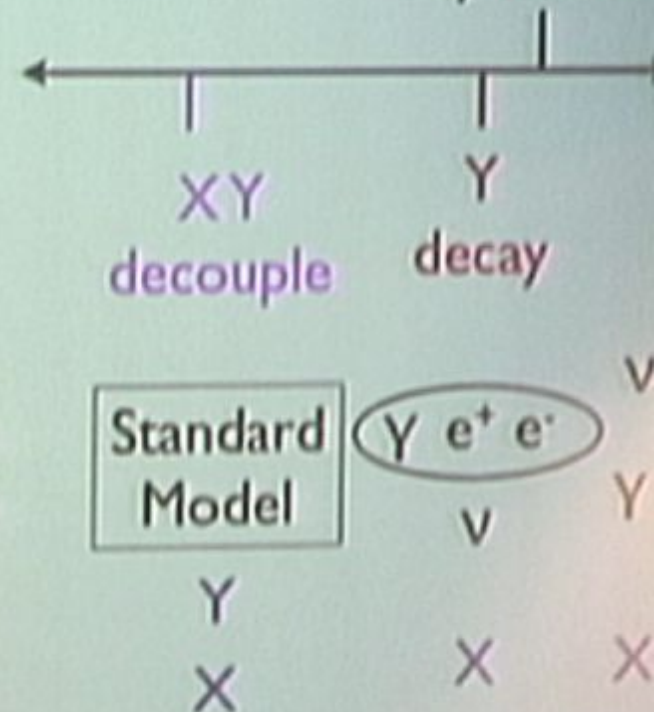
- XY Freezeout:

$$(M T_{\text{hid}})^{3/2} e^{(-M/T_{\text{hid}})} \sigma v \sim (g_* T^4 + T_{\text{hid}}^4)^{1/2} / m_P$$
- WIMP density /entropy ratio n_X/s conserved until Y decay
- entropy $s \sim g_* T^3 + T_{\text{hid}}^3$
- entropy created during Y decay to e^+e^- (or $\mu^+\mu^-$)



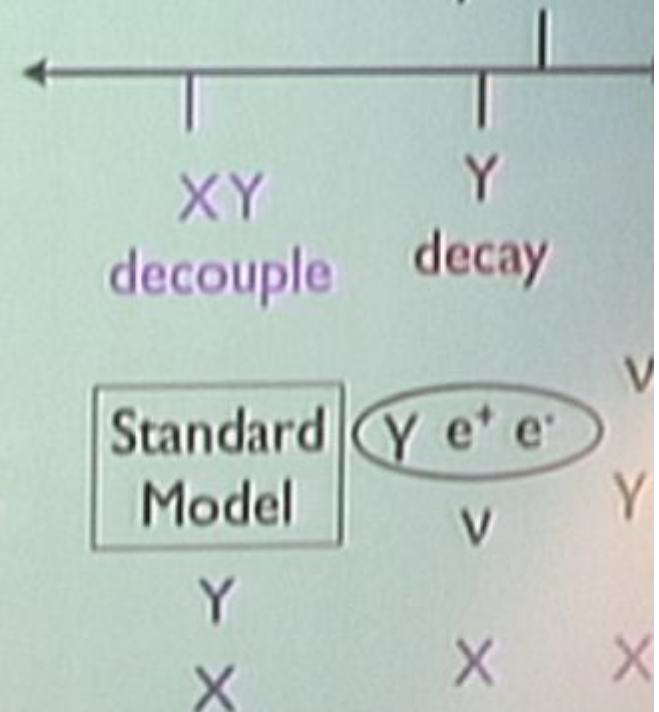
X freezeout and relic X abundance in X-Y(Z) model nucleosynthesis

- XY Freezeout:
 $(M T_{\text{hid}})^{3/2} e^{(-M/T_{\text{hid}})} \sigma v \sim (g_* T^4 + T_{\text{hid}}^4)^{1/2} / m_P$
- WIMP density /entropy ratio n_x/s conserved until Y decay
- entropy $s \sim g_* T^3 + T_{\text{hid}}^3$
- entropy created during Y decay to e^+e^- (or $\mu^+\mu^-$)



X freezeout and relic X abundance in X-Y(Z) model nucleosynthesis

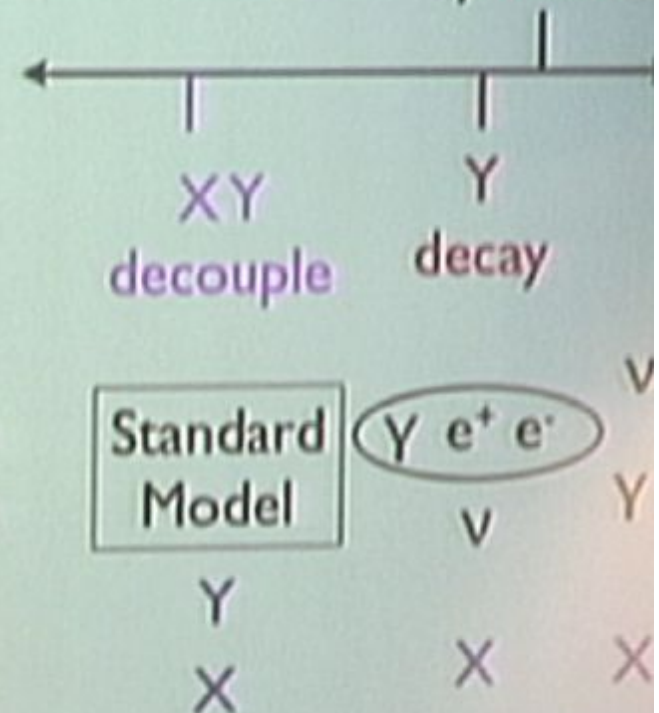
- XY Freezeout:
 $(M T_{\text{hid}})^{3/2} e^{(-M/T_{\text{hid}})} \sigma v \sim (g_* T^4 + T_{\text{hid}}^4)^{1/2} / m_P$
- WIMP density /entropy ratio n_X/s conserved until Y decay
- entropy $s \sim g_* T^3 + T_{\text{hid}}^3$
- entropy created during Y decay to e^+e^- (or $\mu^+\mu^-$)



X freezeout and relic X abundance in X-Y(Z) model nucleosynthesis

- XY Freezeout:

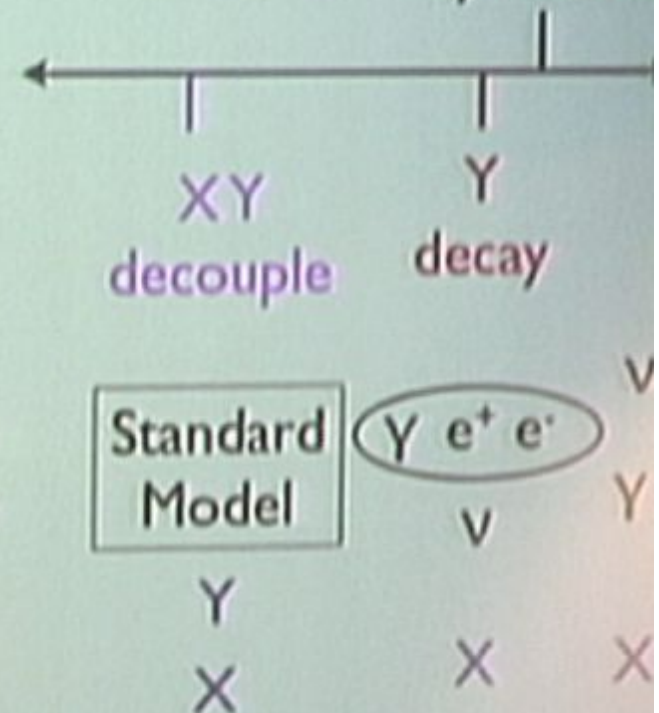
$$(M T_{\text{hid}})^{3/2} e^{(-M/T_{\text{hid}})} \sigma v \sim (g_* T^4 + T_{\text{hid}}^4)^{1/2} / m_P$$
- WIMP density /entropy ratio n_X/s conserved until Y decay
- entropy $s \sim g_* T^3 + T_{\text{hid}}^3$
- entropy created during Y decay to e^+e^- (or $\mu^+\mu^-$)



X freezeout and relic X abundance in X-Y(Z) model nucleosynthesis

- XY Freezeout:

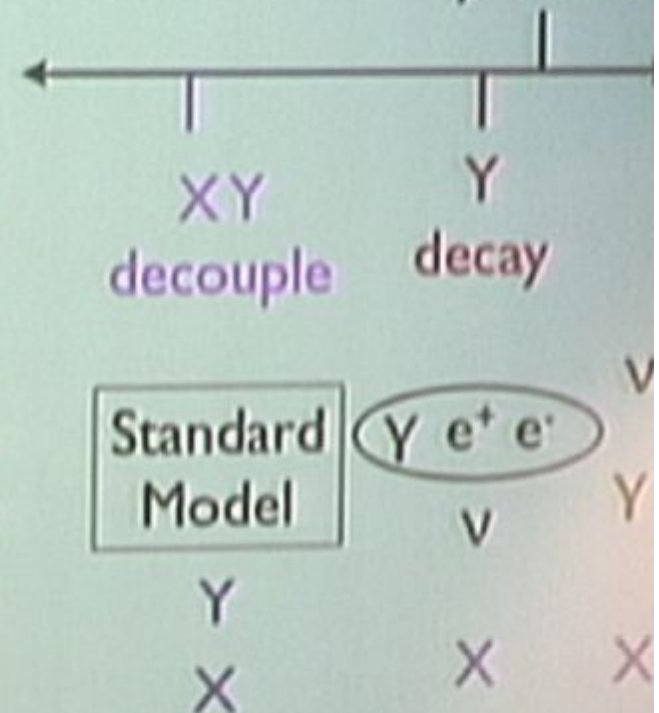
$$(M T_{\text{hid}})^{3/2} e^{(-M/T_{\text{hid}})} \sigma v \sim (g_* T^4 + T_{\text{hid}}^4)^{1/2} / m_P$$
- WIMP density /entropy ratio n_X/s conserved until Y decay
- entropy $s \sim g_* T^3 + T_{\text{hid}}^3$
- entropy created during Y decay to e^+e^- (or $\mu^+\mu^-$)



X freezeout and relic X abundance in X-Y(Z) model nucleosynthesis

- XY Freezeout:

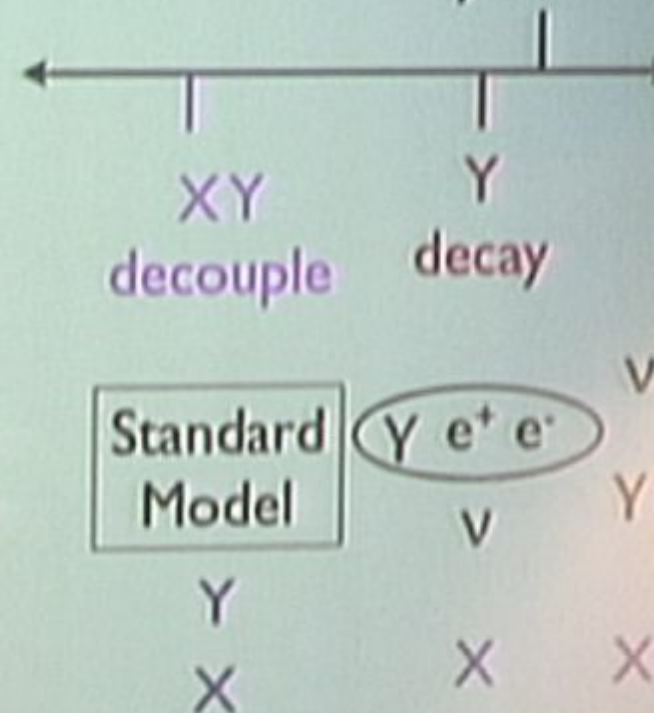
$$(M T_{\text{hid}})^{3/2} e^{(-M/T_{\text{hid}})} \sigma v \sim (g_* T^4 + T_{\text{hid}}^4)^{1/2} / m_P$$
- WIMP density /entropy ratio n_X/s conserved until Y decay
- entropy $s \sim g_* T^3 + T_{\text{hid}}^3$
- entropy created during Y decay to e^+e^- (or $\mu^+\mu^-$)



X freezeout and relic X abundance in X-Y(Z) model nucleosynthesis

- XY Freezeout:

$$(M T_{\text{hid}})^{3/2} e^{(-M/T_{\text{hid}})} \sigma v \sim (g_* T^4 + T_{\text{hid}}^4)^{1/2} / m_P$$
- WIMP density /entropy ratio n_X/s conserved until Y decay
- entropy $s \sim g_* T^3 + T_{\text{hid}}^3$
- entropy created during Y decay to e^+e^- (or $\mu^+\mu^-$)



Freezeout and relic X abundance in X-Y(Z) model

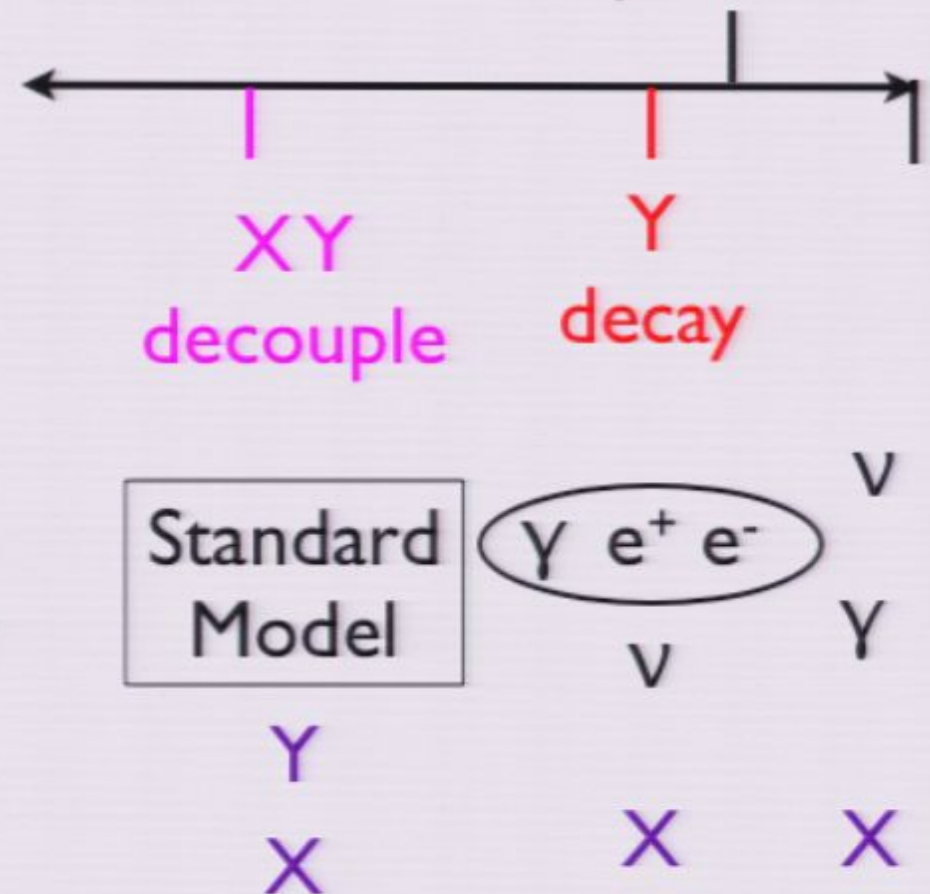
• XY Freezeout:

$$(M T_{\text{hid}})^{3/2} e^{(-M/T_{\text{hid}})} \sigma v \sim (g^* T^4 + T_{\text{hid}}^4)^{1/2} / m_P$$

• WIMP density /entropy ratio n_X/s conserved until Y decay

• entropy $s \sim g^* T^3 + T_{\text{hid}}^3$

• entropy created during Y decay to e^+e^- (or $\mu^+\mu^-$)



- for hidden sector temperature much higher than standard model temp “as if” lower g_* , and so lower entropy during XY freezeout
- $g_* = 86.25$ in SM at 30 GeV, effectively $g_* = 1$ in hidden sector
- less entropy \rightarrow less dilution of dark matter, allow larger M/T , larger $\langle \sigma v \rangle$ for observed relic abundance

- for hidden sector temperature much higher than standard model temp “as if” lower g_* , and so lower entropy during XY freezeout
- $g_* = 86.25$ in SM at 30 GeV, effectively $g_* = 1$ in hidden sector
- less entropy \rightarrow less dilution of dark matter, allow larger M/T , larger $\langle \sigma v \rangle$ for observed relic abundance

- for hidden sector temperature much higher than standard model temp “as if” lower g_* , and so lower entropy during XY freezeout
- $g_* = 86.25$ in SM at 30 GeV, effectively $g_* = 1$ in hidden sector
- less entropy \rightarrow less dilution of dark matter, allow larger M/T , larger $\langle \sigma v \rangle$ for observed relic abundance

$\frac{1}{(0.6 \text{ eV})^2}$
 $\times 10^{-10} \text{ mbn}$

- for hidden sector temperature much higher than standard model temp “as if” lower g_* , and so lower entropy during XY freezeout
- $g_* = 86.25$ in SM at 30 GeV, effectively $g_* = 1$ in hidden sector
- less entropy \rightarrow less dilution of dark matter, allow larger M/T , larger $\langle \sigma v \rangle$ for observed relic abundance

- for hidden sector temperature much higher than standard model temp “as if” lower g_* , and so lower entropy during XY freezeout
- $g_* = 86.25$ in SM at 30 GeV, effectively $g_* = 1$ in hidden sector
- less entropy \rightarrow less dilution of dark matter, allow larger M/T , larger $\langle \sigma v \rangle$ for observed relic abundance

- for hidden sector temperature much higher than standard model temp “as if” lower g_* , and so lower entropy during XY freezeout
- $g_* = 86.25$ in SM at 30 GeV, effectively $g_* = 1$ in hidden sector
- less entropy \rightarrow less dilution of dark matter, allow larger M/T , larger $\langle \sigma v \rangle$ for observed relic abundance

- for hidden sector temperature much higher than standard model temp “as if” lower g_* , and so lower entropy during XY freezeout
- $g_* = 86.25$ in SM at 30 GeV, effectively $g_* = 1$ in hidden sector
- less entropy \rightarrow less dilution of dark matter, allow larger M/T , larger $\langle \sigma v \rangle$ for observed relic abundance

- for hidden sector temperature much higher than standard model temp “as if” lower g_* , and so lower entropy during XY freezeout
- $g_* = 86.25$ in SM at 30 GeV, effectively $g_* = 1$ in hidden sector
- less entropy \rightarrow less dilution of dark matter, allow larger M/T , larger $\langle \sigma v \rangle$ for observed relic abundance

- for hidden sector temperature much higher than standard model temp “as if” lower g_* , and so lower entropy during XY freezeout
- $g_* = 86.25$ in SM at 30 GeV, effectively $g_* = 1$ in hidden sector
- less entropy \rightarrow less dilution of dark matter, allow larger M/T , larger $\langle \sigma v \rangle$ for observed relic abundance

- for hidden sector temperature much higher than standard model temp “as if” lower g_* , and so lower entropy during XY freezeout
- $g_* = 86.25$ in SM at 30 GeV, effectively $g_* = 1$ in hidden sector
- less entropy \rightarrow less dilution of dark matter, allow larger M/T , larger $\langle \sigma v \rangle$ for observed relic abundance

- for hidden sector temperature much higher than standard model temp “as if” lower g_* , and so lower entropy during XY freezeout
- $g_* = 86.25$ in SM at 30 GeV, effectively $g_* = 1$ in hidden sector
- less entropy \rightarrow less dilution of dark matter, allow larger M/T , larger $\langle \sigma v \rangle$ for observed relic abundance

$\frac{1}{(0.6 \text{ eV})^2}$
 $\times 10 \text{ mbn}$

- for hidden sector temperature much higher than standard model temp “as if” lower g_* , and so lower entropy during XY freezeout
- $g_* = 86.25$ in SM at 30 GeV, effectively $g_* = 1$ in hidden sector
- less entropy \rightarrow less dilution of dark matter, allow larger M/T , larger $\langle \sigma v \rangle$ for observed relic abundance

$$\frac{1}{h^2 (eV)^2} \sim 10^{-20}$$

- for hidden sector temperature much higher than standard model temp “as if” lower g_* , and so lower entropy during XY freezeout
- $g_* = 86.25$ in SM at 30 GeV, effectively $g_* = 1$ in hidden sector
- less entropy \rightarrow less dilution of dark matter, allow larger M/T , larger $\langle \sigma v \rangle$ for observed relic abundance

$$\frac{1}{(5 \text{ GeV})^2} \sim 10^{-20}$$

- for hidden sector temperature much higher than standard model temp “as if” lower g_* , and so lower entropy during XY freezeout
- $g_* = 86.25$ in SM at 30 GeV, effectively $g_* = 1$ in hidden sector
- less entropy \rightarrow less dilution of dark matter, allow larger M/T , larger $\langle \sigma v \rangle$ for observed relic abundance

$$\frac{1}{(6 \text{ eV})^2}$$

$$\frac{1}{\sigma h} \times 10^{-20}$$

- for hidden sector temperature much higher than standard model temp “as if” lower g_* , and so lower entropy during XY freezeout
- $g_* = 86.25$ in SM at 30 GeV, effectively $g_* = 1$ in hidden sector
- less entropy \rightarrow less dilution of dark matter, allow larger M/T , larger $\langle \sigma v \rangle$ for observed relic abundance

- for hidden sector temperature much higher than standard model temp “as if” lower g_* , and so lower entropy during XY freezeout
- $g_* = 86.25$ in SM at 30 GeV, effectively $g_* = 1$ in hidden sector
- less entropy \rightarrow less dilution of dark matter, allow larger M/T , larger $\langle \sigma v \rangle$ for observed relic abundance

$$\frac{1}{(0.6 \text{ eV})^2}$$

$$mbn \times 10^{-2}$$

Entropy created

- for late decaying Y (temp ~ 100 MeV) g^* in visible sector = 10.75
- In “sudden decay” approximation, visible sector gets suddenly reheated.
- If Y particle is relativistic, entropy increases by factor of $\sim 15.25^{1/4}$
- annihilation cross section larger than in standard WIMP scenario by factor as big as $86.25^{1/2}/15.25^{1/4} \sim 5$

Entropy created

- for late decaying Y (temp ~ 100 MeV) g_* in visible sector = 10.75
- In “sudden decay” approximation, visible sector gets suddenly reheated.
- If Y particle is relativistic, entropy increases by factor of $\sim 15.25^{1/4}$
- annihilation cross section larger than in standard WIMP scenario by factor as big as $86.25^{1/2}/15.25^{1/4} \sim 5$

Entropy created

- for late decaying Y (temp ~ 100 MeV) g_* in visible sector = 10.75
- In “sudden decay” approximation, visible sector gets suddenly reheated.
- If Y particle is relativistic, entropy increases by factor of $\sim 15.25^{1/4}$
- annihilation cross section larger than in standard WIMP scenario by factor as big as $86.25^{1/2}/15.25^{1/4} \sim 5$

Entropy created

- for late decaying Y (temp ~ 100 MeV) g_* in visible sector = 10.75
- In “sudden decay” approximation, visible sector gets suddenly reheated.
- If Y particle is relativistic, entropy increases by factor of $\sim 15.25^{1/4}$
- annihilation cross section larger than in standard WIMP scenario by factor as big as $86.25^{1/2}/15.25^{1/4} \sim 5$

Entropy created

- for late decaying Y (temp ~ 100 MeV) g^* in visible sector = 10.75
- In “sudden decay” approximation, visible sector gets suddenly reheated.
- If Y particle is relativistic, entropy increases by factor of $\sim 15.25^{1/4}$
- annihilation cross section larger than in standard WIMP scenario by factor as big as $86.25^{1/2}/15.25^{1/4} \sim 5$

X annihilation rate

- standard WIMP; for $M \sim 100$ GeV, correct abundance for $M/T_{\text{freeze}} \sim 20$ (varies as $\log(M)$)
- $\langle \sigma v \rangle \sim 3 \times 10^{-26} \text{ cm}^3/\text{s}$ gives observed relic abundance for standard WIMP
- factor of $86.25^{1/2}/15.25^{1/4}$ can increase annihilation cross section to
 $\langle \sigma v \rangle \sim 1.5 \times 10^{-25} \text{ cm}^3/\text{s}$
- still need large astrophysical boost factor (40) or Sommerfeld enhancement to explain ATIC

X annihilation rate

- standard WIMP; for $M \sim 100$ GeV, correct abundance for $M/T_{\text{freeze}} \sim 20$ (varies as $\log(M)$)
- $\langle \sigma v \rangle \sim 3 \times 10^{-26} \text{ cm}^3/\text{s}$ gives observed relic abundance for standard WIMP
- factor of $86.25^{1/2}/15.25^{1/4}$ can increase annihilation cross section to $\langle \sigma v \rangle \sim 1.5 \times 10^{-25} \text{ cm}^3/\text{s}$
- still need large astrophysical boost factor (40) or Sommerfeld enhancement to explain ATIC

X annihilation rate

- standard WIMP; for $M \sim 100$ GeV, correct abundance for $M/T_{\text{freeze}} \sim 20$ (varies as $\log(M)$)
- $\langle \sigma v \rangle \sim 3 \times 10^{-26} \text{ cm}^3/\text{s}$ gives observed relic abundance for standard WIMP
- factor of $86.25^{1/2}/15.25^{1/4}$ can increase annihilation cross section to $\langle \sigma v \rangle \sim 1.5 \times 10^{-25} \text{ cm}^3/\text{s}$
- still need large astrophysical boost factor (40) or Sommerfeld enhancement to explain ATIC

X annihilation rate

- standard WIMP; for $M \sim 100$ GeV, correct abundance for $M/T_{\text{freeze}} \sim 20$ (varies as $\log(M)$)
- $\langle \sigma v \rangle \sim 3 \times 10^{-26} \text{ cm}^3/\text{s}$ gives observed relic abundance for standard WIMP
- factor of $86.25^{1/2}/15.25^{1/4}$ can increase annihilation cross section to $\langle \sigma v \rangle \sim 1.5 \times 10^{-25} \text{ cm}^3/\text{s}$
- still need large astrophysical boost factor (40) or Sommerfeld enhancement to explain ATIC

X annihilation rate

- standard WIMP; for $M \sim 100$ GeV, correct abundance for $M/T_{\text{freeze}} \sim 20$ (varies as $\log(M)$)
- $\langle \sigma v \rangle \sim 3 \times 10^{-26} \text{ cm}^3/\text{s}$ gives observed relic abundance for standard WIMP
- factor of $86.25^{1/2}/15.25^{1/4}$ can increase annihilation cross section to $\langle \sigma v \rangle \sim 1.5 \times 10^{-25} \text{ cm}^3/\text{s}$
- still need large astrophysical boost factor (40) or Sommerfeld enhancement to explain ATIC

X annihilation rate

- standard WIMP; for $M \sim 100$ GeV, correct abundance for $M/T_{\text{freeze}} \sim 20$ (varies as $\log(M)$)
- $\langle \sigma v \rangle \sim 3 \times 10^{-26} \text{ cm}^3/\text{s}$ gives observed relic abundance for standard WIMP
- factor of $86.25^{1/2}/15.25^{1/4}$ can increase annihilation cross section to $\langle \sigma v \rangle \sim 1.5 \times 10^{-25} \text{ cm}^3/\text{s}$
- still need large astrophysical boost factor (40) or Sommerfeld enhancement to explain ATIC

X annihilation rate

- standard WIMP; for $M \sim 100$ GeV, correct abundance for $M/T_{\text{freeze}} \sim 20$ (varies as $\log(M)$)
- $\langle \sigma v \rangle \sim 3 \times 10^{-26} \text{ cm}^3/\text{s}$ gives observed relic abundance for standard WIMP
- factor of $86.25^{1/2}/15.25^{1/4}$ can increase annihilation cross section to $\langle \sigma v \rangle \sim 1.5 \times 10^{-25} \text{ cm}^3/\text{s}$
- still need large astrophysical boost factor (40) or Sommerfeld enhancement to explain ATIC

X annihilation rate

- standard WIMP; for $M \sim 100$ GeV, correct abundance for $M/T_{\text{freeze}} \sim 20$ (varies as $\log(M)$)
- $\langle \sigma v \rangle \sim 3 \times 10^{-26} \text{ cm}^3/\text{s}$ gives observed relic abundance for standard WIMP
- factor of $86.25^{1/2}/15.25^{1/4}$ can increase annihilation cross section to $\langle \sigma v \rangle \sim 1.5 \times 10^{-25} \text{ cm}^3/\text{s}$
- still need large astrophysical boost factor (40) or Sommerfeld enhancement to explain ATIC

X annihilation rate

- standard WIMP; for $M \sim 100$ GeV, correct abundance for $M/T_{\text{freeze}} \sim 20$ (varies as $\log(M)$)
- $\langle \sigma v \rangle \sim 3 \times 10^{-26} \text{ cm}^3/\text{s}$ gives observed relic abundance for standard WIMP
- factor of $86.25^{1/2}/15.25^{1/4}$ can increase annihilation cross section to $\langle \sigma v \rangle \sim 1.5 \times 10^{-25} \text{ cm}^3/\text{s}$
- still need large astrophysical boost factor (40) or Sommerfeld enhancement to explain ATIC

X annihilation rate

- standard WIMP; for $M \sim 100$ GeV, correct abundance for $M/T_{\text{freeze}} \sim 20$ (varies as $\log(M)$)
- $\langle \sigma v \rangle \sim 3 \times 10^{-26} \text{ cm}^3/\text{s}$ gives observed relic abundance for standard WIMP
- factor of $86.25^{1/2}/15.25^{1/4}$ can increase annihilation cross section to $\langle \sigma v \rangle \sim 1.5 \times 10^{-25} \text{ cm}^3/\text{s}$
- still need large astrophysical boost factor (40) or Sommerfeld enhancement to explain ATIC

X annihilation rate

- standard WIMP; for $M \sim 100$ GeV, correct abundance for $M/T_{\text{freeze}} \sim 20$ (varies as $\log(M)$)
- $\langle \sigma v \rangle \sim 3 \times 10^{-26} \text{ cm}^3/\text{s}$ gives observed relic abundance for standard WIMP
- factor of $86.25^{1/2}/15.25^{1/4}$ can increase annihilation cross section to $\langle \sigma v \rangle \sim 1.5 \times 10^{-25} \text{ cm}^3/\text{s}$
- still need large astrophysical boost factor (40) or Sommerfeld enhancement to explain ATIC

X annihilation rate

- standard WIMP; for $M \sim 100$ GeV, correct abundance for $M/T_{\text{freeze}} \sim 20$ (varies as $\log(M)$)
- $\langle \sigma v \rangle \sim 3 \times 10^{-26} \text{ cm}^3/\text{s}$ gives observed relic abundance for standard WIMP
- factor of $86.25^{1/2}/15.25^{1/4}$ can increase annihilation cross section to $\langle \sigma v \rangle \sim 1.5 \times 10^{-25} \text{ cm}^3/\text{s}$
- still need large astrophysical boost factor (40) or Sommerfeld enhancement to explain ATIC

X annihilation rate

- standard WIMP; for $M \sim 100$ GeV, correct abundance for $M/T_{\text{freeze}} \sim 20$ (varies as $\log(M)$)
- $\langle \sigma v \rangle \sim 3 \times 10^{-26} \text{ cm}^3/\text{s}$ gives observed relic abundance for standard WIMP
- factor of $86.25^{1/2}/15.25^{1/4}$ can increase annihilation cross section to $\langle \sigma v \rangle \sim 1.5 \times 10^{-25} \text{ cm}^3/\text{s}$
- still need large astrophysical boost factor (40) or Sommerfeld enhancement to explain ATIC

X annihilation rate

- standard WIMP; for $M \sim 100$ GeV, correct abundance for $M/T_{\text{freeze}} \sim 20$ (varies as $\log(M)$)
- $\langle \sigma v \rangle \sim 3 \times 10^{-26} \text{ cm}^3/\text{s}$ gives observed relic abundance for standard WIMP
- factor of $86.25^{1/2}/15.25^{1/4}$ can increase annihilation cross section to
 $\langle \sigma v \rangle \sim 1.5 \times 10^{-25} \text{ cm}^3/\text{s}$
- still need large astrophysical boost factor (40) or Sommerfeld enhancement to explain ATIC

X annihilation rate

- standard WIMP; for $M \sim 100$ GeV, correct abundance for $M/T_{\text{freeze}} \sim 20$ (varies as $\log(M)$)
- $\langle \sigma v \rangle \sim 3 \times 10^{-26} \text{ cm}^3/\text{s}$ gives observed relic abundance for standard WIMP
- factor of $86.25^{1/2}/15.25^{1/4}$ can increase annihilation cross section to $\langle \sigma v \rangle \sim 1.5 \times 10^{-25} \text{ cm}^3/\text{s}$
- still need large astrophysical boost factor (40) or Sommerfeld enhancement to explain ATIC

X annihilation rate

- standard WIMP; for $M \sim 100$ GeV, correct abundance for $M/T_{\text{freeze}} \sim 20$ (varies as $\log(M)$)
- $\langle \sigma v \rangle \sim 3 \times 10^{-26} \text{ cm}^3/\text{s}$ gives observed relic abundance for standard WIMP
- factor of $86.25^{1/2}/15.25^{1/4}$ can increase annihilation cross section to $\langle \sigma v \rangle \sim 1.5 \times 10^{-25} \text{ cm}^3/\text{s}$
- still need large astrophysical boost factor (40) or Sommerfeld enhancement to explain ATIC

X annihilation rate

- standard WIMP; for $M \sim 100$ GeV, correct abundance for $M/T_{\text{freeze}} \sim 20$ (varies as $\log(M)$)
- $\langle \sigma v \rangle \sim 3 \times 10^{-26} \text{ cm}^3/\text{s}$ gives observed relic abundance for standard WIMP
- factor of $86.25^{1/2}/15.25^{1/4}$ can increase annihilation cross section to $\langle \sigma v \rangle \sim 1.5 \times 10^{-25} \text{ cm}^3/\text{s}$
- still need large astrophysical boost factor (40) or Sommerfeld enhancement to explain ATIC

X annihilation rate

- standard WIMP; for $M \sim 100$ GeV, correct abundance for $M/T_{\text{freeze}} \sim 20$ (varies as $\log(M)$)
- $\langle \sigma v \rangle \sim 3 \times 10^{-26} \text{ cm}^3/\text{s}$ gives observed relic abundance for standard WIMP
- factor of $86.25^{1/2}/15.25^{1/4}$ can increase annihilation cross section to $\langle \sigma v \rangle \sim 1.5 \times 10^{-25} \text{ cm}^3/\text{s}$
- still need large astrophysical boost factor (40) or Sommerfeld enhancement to explain ATIC

X annihilation rate

- standard WIMP; for $M \sim 100$ GeV, correct abundance for $M/T_{\text{freeze}} \sim 20$ (varies as $\log(M)$)
- $\langle \sigma v \rangle \sim 3 \times 10^{-26} \text{ cm}^3/\text{s}$ gives observed relic abundance for standard WIMP
- factor of $86.25^{1/2}/15.25^{1/4}$ can increase annihilation cross section to $\langle \sigma v \rangle \sim 1.5 \times 10^{-25} \text{ cm}^3/\text{s}$
- still need large astrophysical boost factor (40) or Sommerfeld enhancement to explain ATIC

WIMP Relic Abundance Summary

- WIMP abundance determined by X-Y nonequilibrium
- hidden sector (X,Y) temp different from visible sector
- visible sector reheated by Y decays before nucleosynthesis
- allows for annihilation cross section to be enhanced relative to traditional relic abundance calculation by factor of < 5 , increases indirect detection prospects
- Kinematic constraint explains why Y primarily decays to e^+e^- (some $\Upsilon\Upsilon$ possible)

WIMP Relic Abundance Summary

- WIMP abundance determined by X-Y nonequilibrium
- hidden sector (X,Y) temp different from visible sector
- visible sector reheated by Y decays before nucleosynthesis
- allows for annihilation cross section to be enhanced relative to traditional relic abundance calculation by factor of < 5 , increases indirect detection prospects
- Kinematic constraint explains why Y primarily decays to e^+e^- (some $\gamma\gamma$ possible)

$$\frac{1}{(0.6 \text{ eV})^2} \\ \text{mbn} \times 10^{-20}$$

WIMP Relic Abundance Summary

- WIMP abundance determined by X-Y nonequilibrium
- hidden sector (X,Y) temp different from visible sector
- visible sector reheated by Y decays before nucleosynthesis
- allows for annihilation cross section to be enhanced relative to traditional relic abundance calculation by factor of < 5 , increases indirect detection prospects
- Kinematic constraint explains why Y primarily decays to e^+e^- (some $\gamma\gamma$ possible)

WIMP Relic Abundance Summary

- WIMP abundance determined by X-Y nonequilibrium
- hidden sector (X,Y) temp different from visible sector
- visible sector reheated by Y decays before nucleosynthesis
- allows for annihilation cross section to be enhanced relative to traditional relic abundance calculation by factor of < 5 , increases indirect detection prospects
- Kinematic constraint explains why Y primarily decays to e^+e^- (some $\gamma\gamma$ possible)

WIMP Relic Abundance Summary

- WIMP abundance determined by X-Y nonequilibrium
- hidden sector (X,Y) temp different from visible sector
- visible sector reheated by Y decays before nucleosynthesis
- allows for annihilation cross section to be enhanced relative to traditional relic abundance calculation by factor of < 5 , increases indirect detection prospects
- Kinematic constraint explains why Y primarily decays to e^+e^- (some $\gamma\gamma$ possible)

WIMP Relic Abundance Summary

- WIMP abundance determined by X-Y nonequilibrium
- hidden sector (X,Y) temp different from visible sector
- visible sector reheated by Y decays before nucleosynthesis
- allows for annihilation cross section to be enhanced relative to traditional relic abundance calculation by factor of < 5 , increases indirect detection prospects
- Kinematic constraint explains why Y primarily decays to e^+e^- (some $\gamma\gamma$ possible)

WIMP Relic Abundance Summary

- WIMP abundance determined by X-Y nonequilibrium
- hidden sector (X,Y) temp different from visible sector
- visible sector reheated by Y decays before nucleosynthesis
- allows for annihilation cross section to be enhanced relative to traditional relic abundance calculation by factor of < 5 , increases indirect detection prospects
- Kinematic constraint explains why Y primarily decays to e^+e^- (some $\gamma\gamma$ possible)

WIMP Relic Abundance Summary

- WIMP abundance determined by X-Y nonequilibrium
- hidden sector (X,Y) temp different from visible sector
- visible sector reheated by Y decays before nucleosynthesis
- allows for annihilation cross section to be enhanced relative to traditional relic abundance calculation by factor of < 5 , increases indirect detection prospects
- Kinematic constraint explains why Y primarily decays to e^+e^- (some $\gamma\gamma$ possible)

WIMP Relic Abundance Summary

- WIMP abundance determined by X-Y nonequilibrium
- hidden sector (X,Y) temp different from visible sector
- visible sector reheated by Y decays before nucleosynthesis
- allows for annihilation cross section to be enhanced relative to traditional relic abundance calculation by factor of < 5 , increases indirect detection prospects
- Kinematic constraint explains why Y primarily decays to e^+e^- (some $\gamma\gamma$ possible)

$$\frac{1}{(0.6 \text{ eV})^2} \times 10^{-20} \text{ mbn}$$

For $Y \rightarrow e^+, e^-$ Injection Energy Spectrum in galactic frame

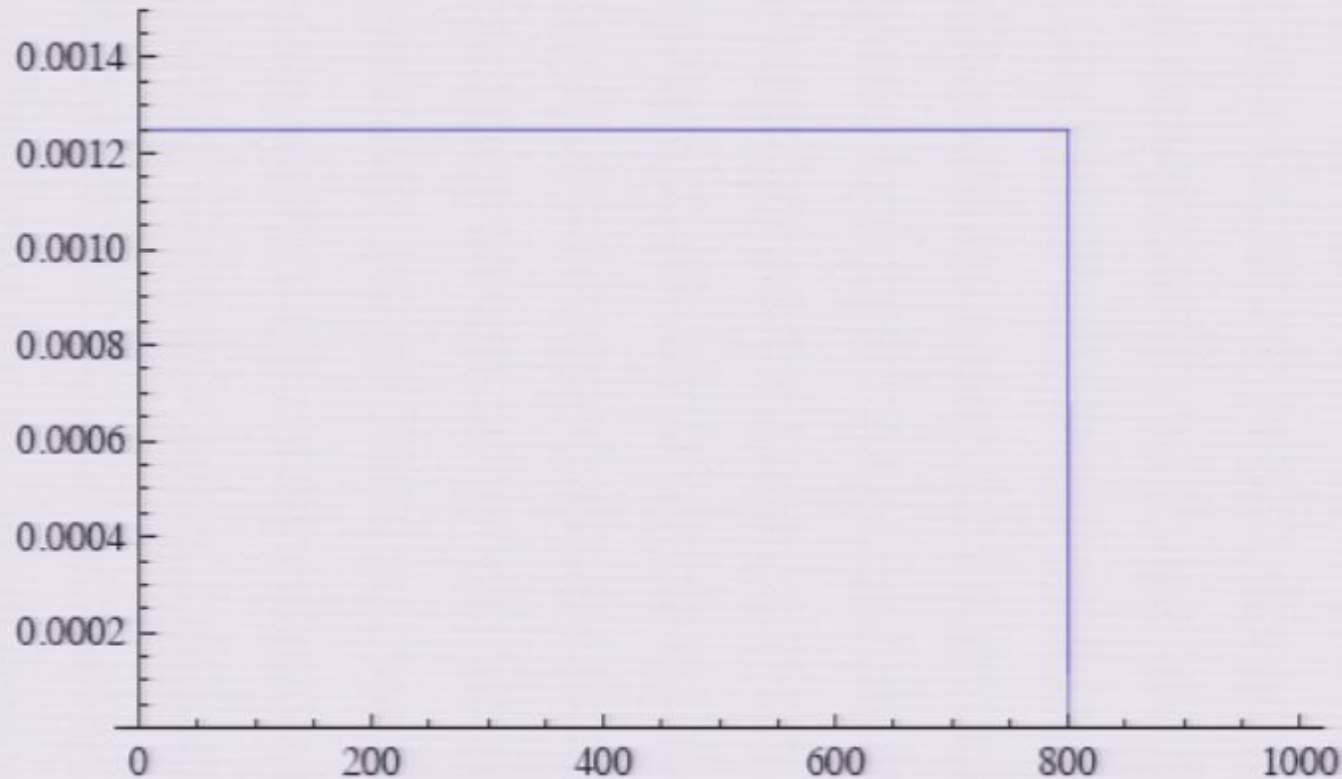


FIG. 2: The energy spectrum dN/dE of the electrons as a function of the lab frame energy for $M=800\text{GeV}$, $m=200\text{MeV}$

Galactic propagation

- Source of positrons proportional to density²
- Various models for density profile make small difference compared with other unknowns
- inject into diffusion model for galaxy which has various not precisely known parameters and “boost factor” B to account for nearby substructure
- fit parameters within range $B < 20$

Excess of Cosmic positrons?

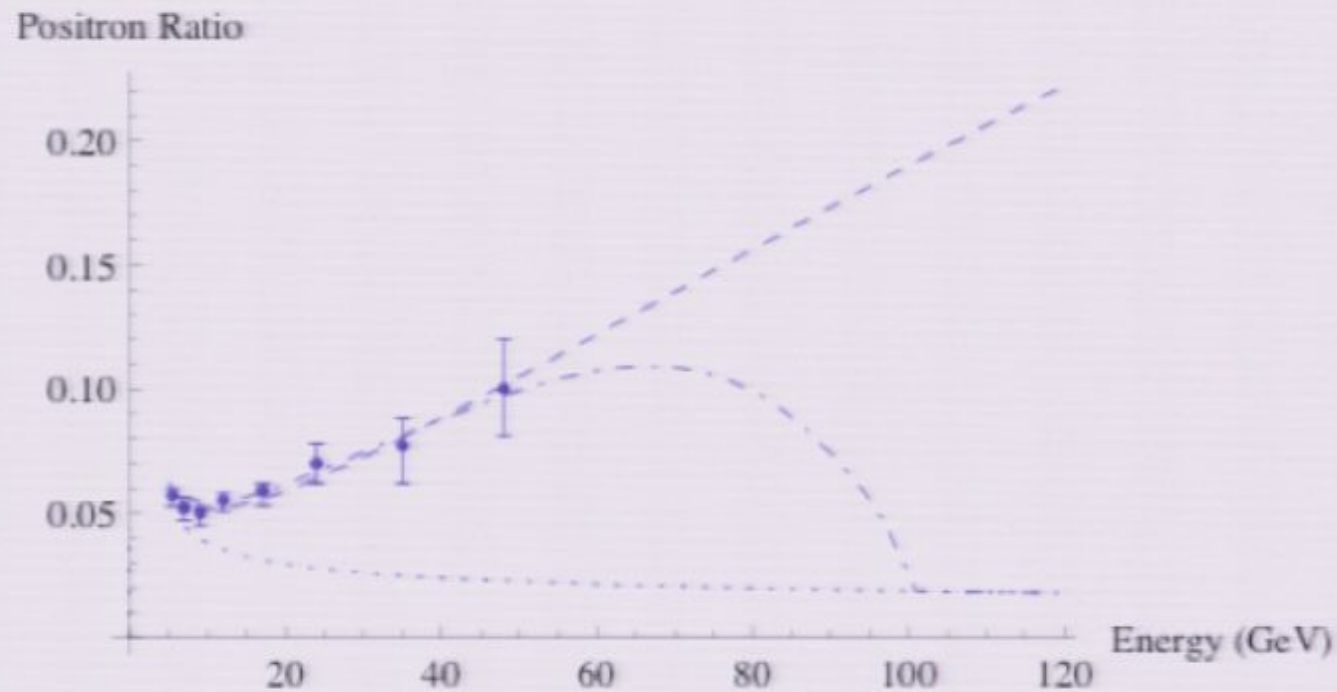


FIG. 2: Positron excess below 100GeV shown against the preliminary PAMELA data. The dash-dot curve is $M = 100$ GeV. The dashed curve is $M = 800$ GeV. The bottom dotted line is the background level.

Excess of Cosmic positrons?

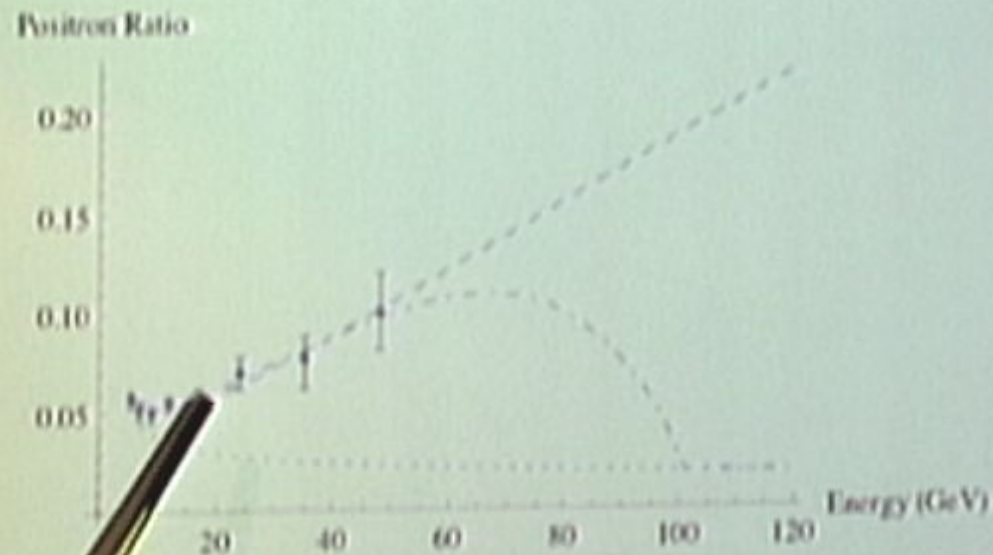


FIG. 2: Positron excess below 100GeV shown against the preliminary PAMELA data. The dash-dot curve is $M = 51$ GeV. The dashed curve is $M = 800$ GeV. The bottom dotted line is the background level.

Excess of Cosmic positrons?

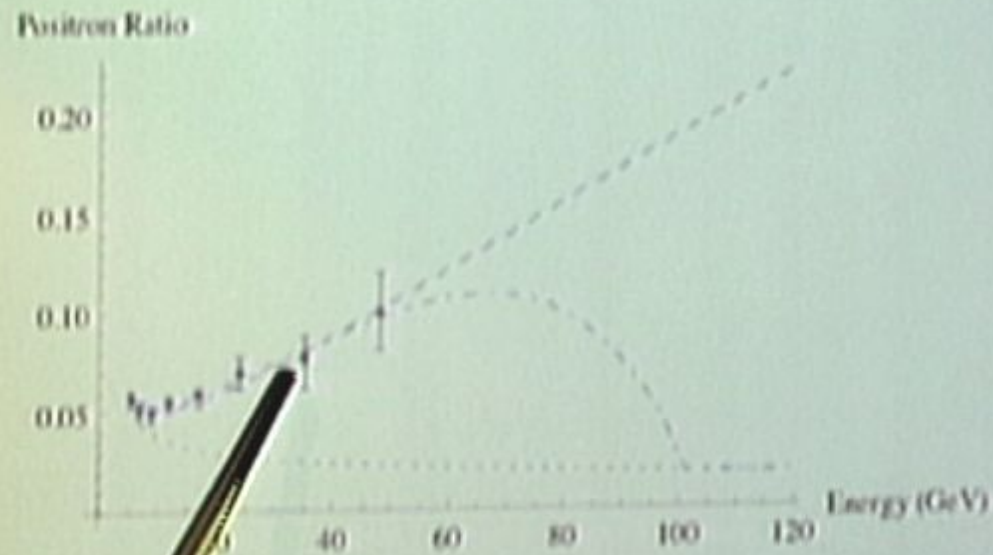


FIG. 2: Positron excess below 100GeV shown against the preliminary PAMELA data. The dash-dot curve is $M = 100 \text{ GeV}$. The dashed curve is $M = 800 \text{ GeV}$. The bottom dotted line is the background level.

Excess of Cosmic positrons?

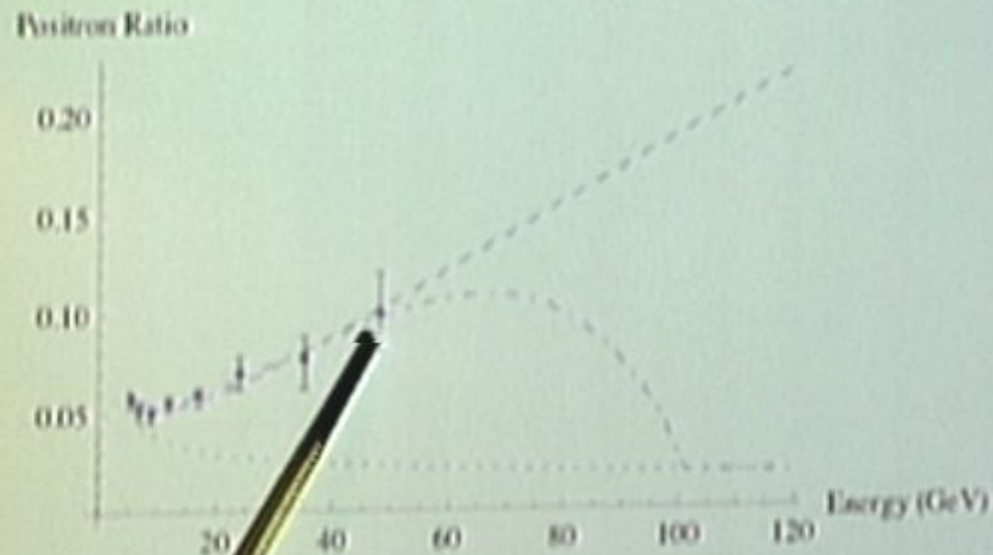


FIG. 2: Positron excess below 100GeV shown against the preliminary PAMELA data. The dash-dot curve is $M = 100$ GeV. The dashed curve is $M = 800$ GeV. The bottom dotted line is the background level.

Excess of Cosmic positrons?

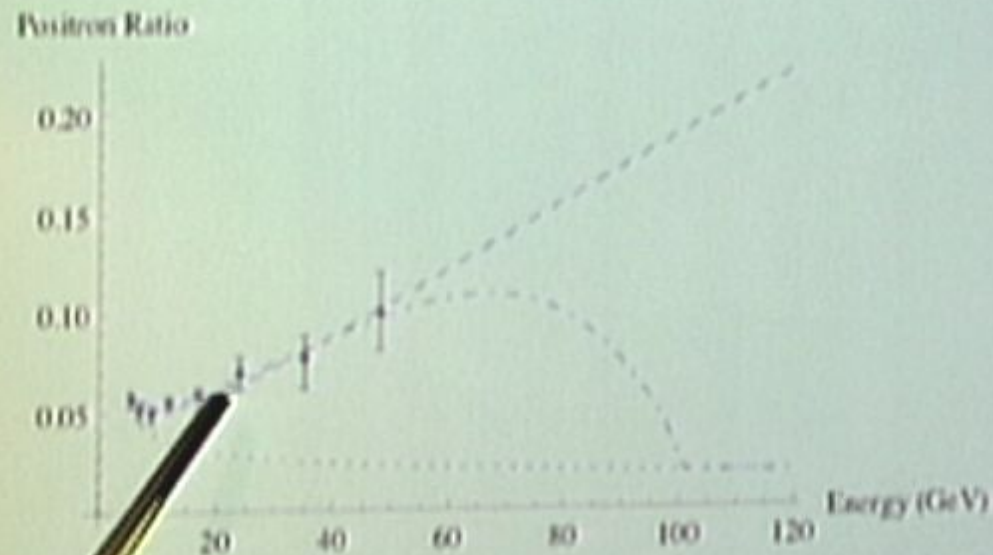


FIG. 2: Positron excess below 100 GeV shown against the preliminary PAMELA data. The dash-dot curve is $M = 50$ GeV. The dashed curve is $M = 800$ GeV. The bottom dotted line is the background level.

Excess of Cosmic positrons?

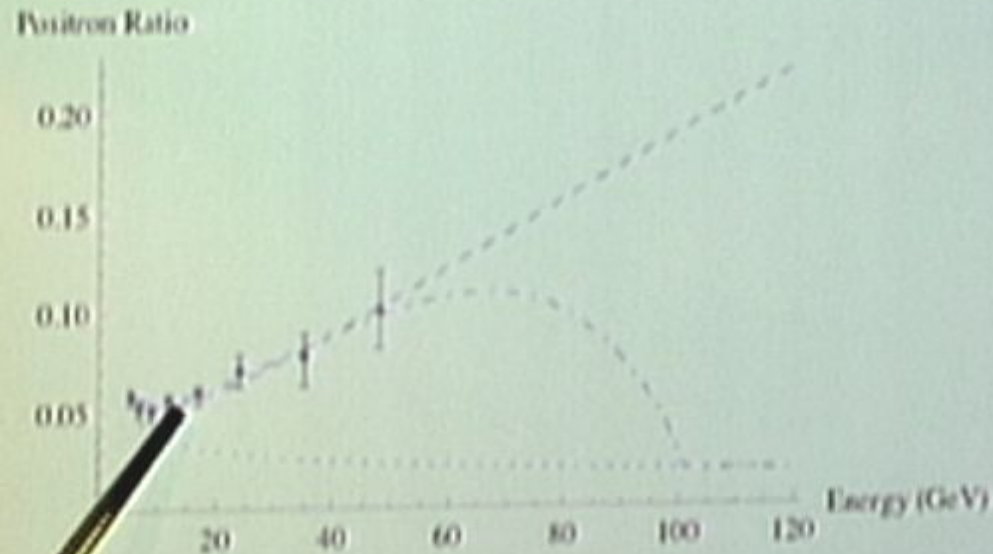


Fig. 2: Positron excess below 100GeV shown against the preliminary PAMELA data. The dash-dot curve is $M = 100$ GeV. The dashed curve is $M = 800$ GeV. The bottom dotted line is the background level.

Excess of Cosmic positrons?

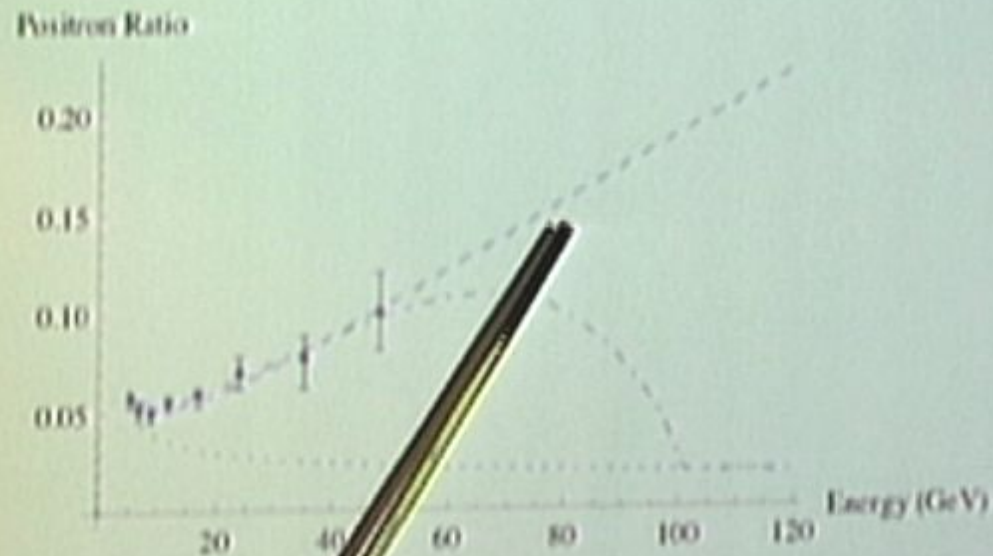


FIG. 2: Positron excess below 100 GeV shown against the preliminary PAMELA data. The dash-dot curve is $M = 100$ GeV. The dashed curve is $M = 800$ GeV. The bottom dotted line is the background level.

Excess of Cosmic positrons?

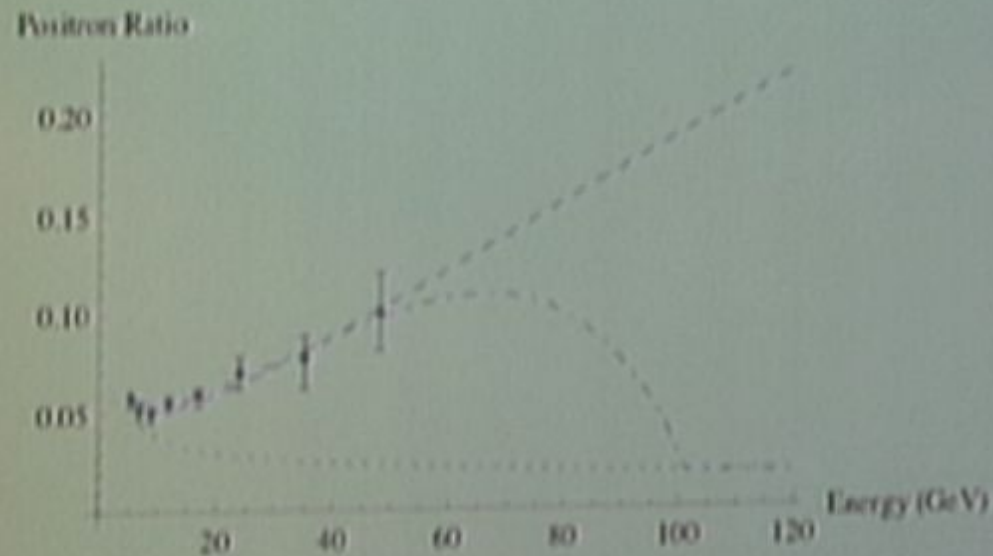


FIG. 2: Positron excess below 100GeV shown against the preliminary PAMELA data. The dash-dot curve is $M = 100$ GeV. The dashed curve is $M = 800$ GeV. The bottom dotted line is the background level.

Excess of Cosmic positrons?

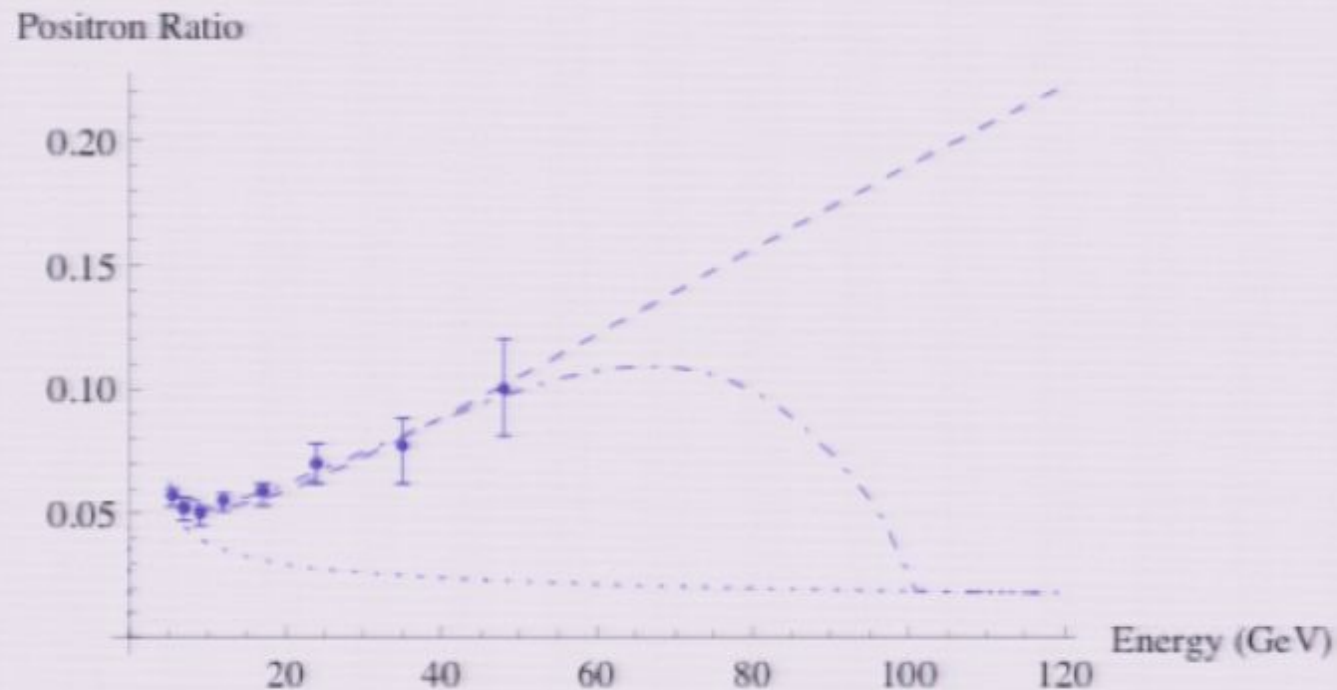


FIG. 2: Positron excess below 100GeV shown against the preliminary PAMELA data. The dash-dot curve is $M = 100$ GeV. The dashed curve is $M = 800$ GeV. The bottom dotted line is the background level.

ATIC Feature in Cosmic Electron Spectrum?

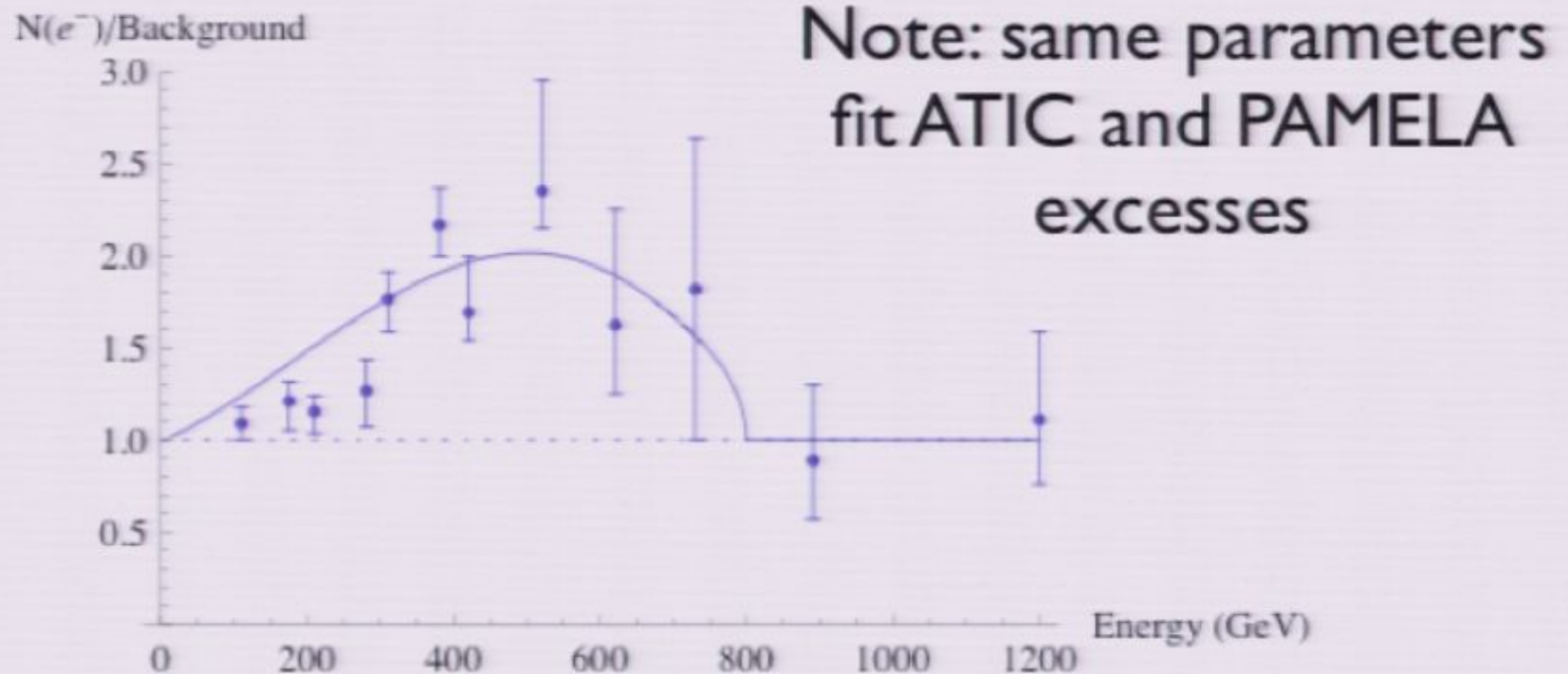
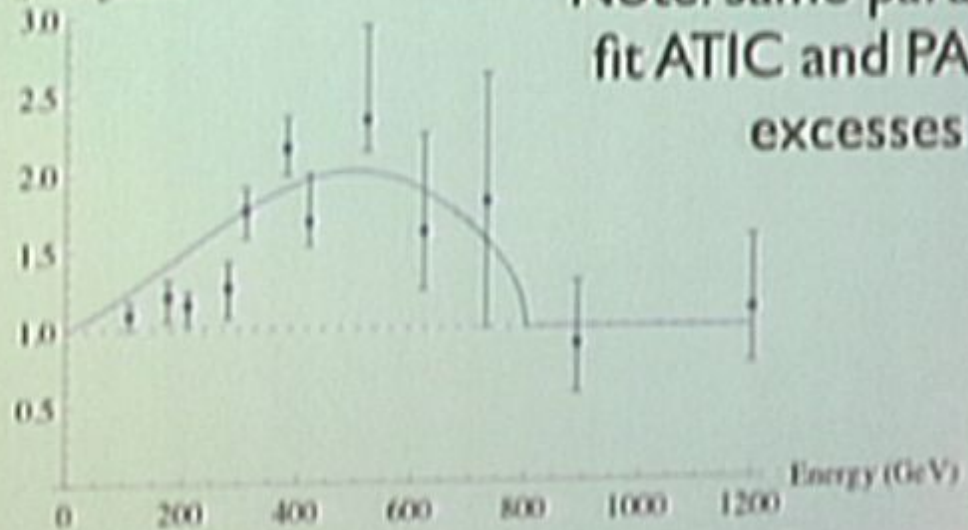


FIG. 3: Ratio of number of electrons to number of background electrons show against the ATIC data for $M = 800$ GeV. The dotted line is the background level, fixed to be 1 in this ratio.

ATIC Feature in Cosmic Electron Spectrum?

$N(e^-)/\text{Background}$



Note: same parameters
fit ATIC and PAMELA
excesses

FIG. 3: Ratio of number of electrons to number of background electrons show against the ATIC data for $M = 800$ GeV. The dotted line is the background level, fixed to be 1 in this ratio.

ATIC Feature in Cosmic Electron Spectrum?

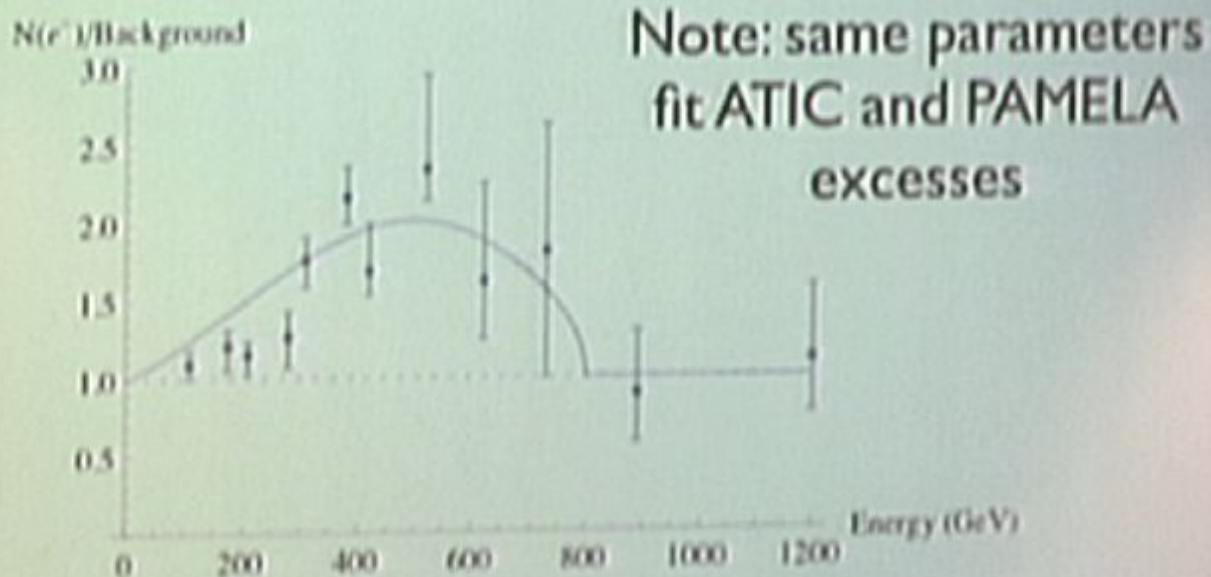


FIG. 3: Ratio of number of electrons to number of background electrons show against the ATIC data for $M = 800$ GeV. The dotted line is the background level, fixed to be 1 in this ratio.

ATIC Feature in Cosmic Electron Spectrum?

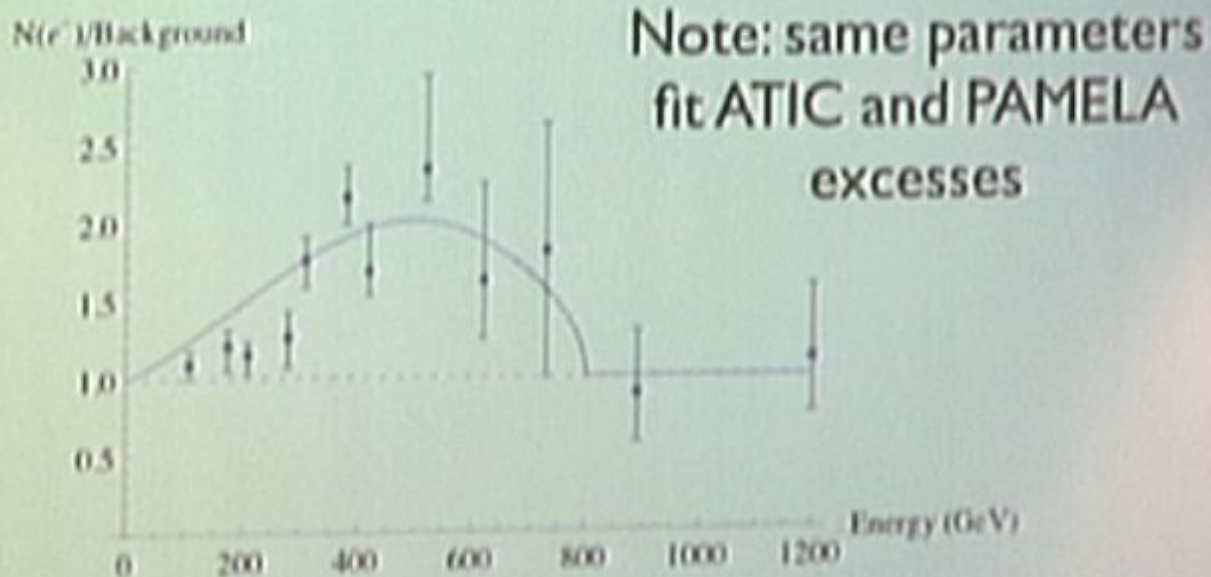


FIG. 3: Ratio of number of electrons to number of background electrons show against the ATIC data for $M = 800$ GeV. The dotted line is the background level, fixed to be 1 in this ratio.

ATIC Feature in Cosmic Electron Spectrum?

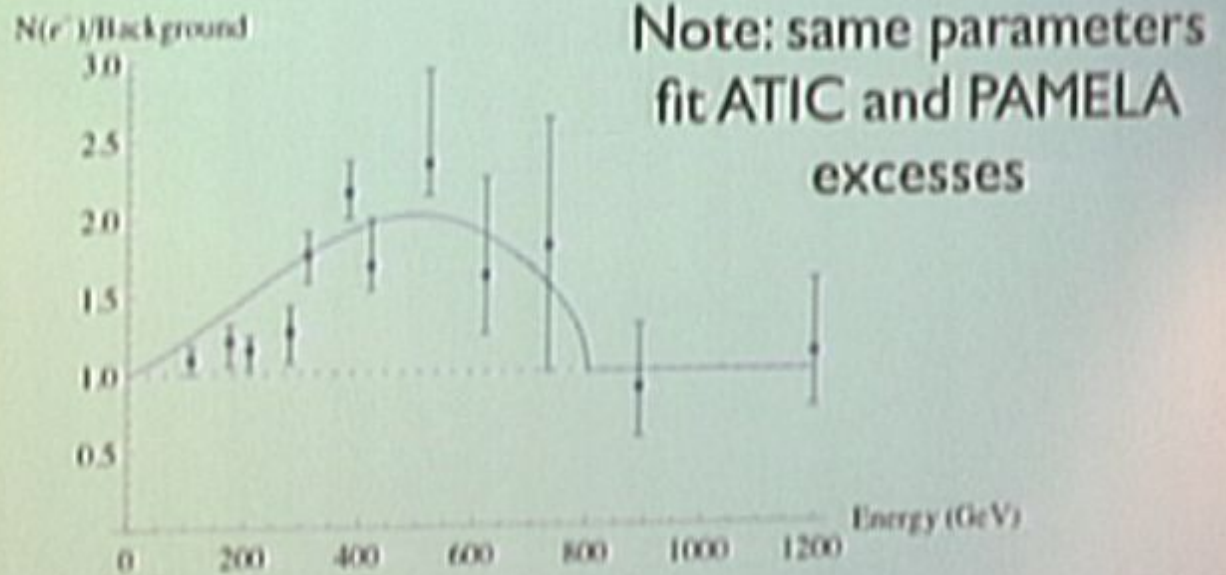


FIG. 3: Ratio of number of electrons to number of background electrons show against the ATIC data for $M = 800$ GeV. The dotted line is the background level, fixed to be 1 in this ratio.

ATIC Feature in Cosmic Electron Spectrum?

$N(e^-)/\text{Background}$

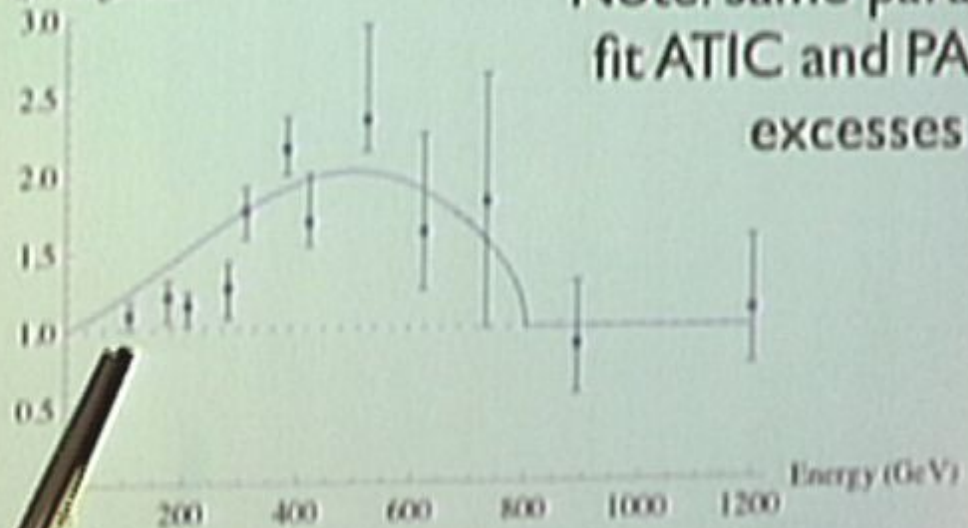


FIG. 1. Ratio of number of electrons to number of background electrons show against the ATIC data for $M = 800$ GeV. The dashed line is the background level, fixed to be 1 in this ratio.

ATIC Feature in Cosmic Electron Spectrum?

$N(e^-)/\text{Background}$

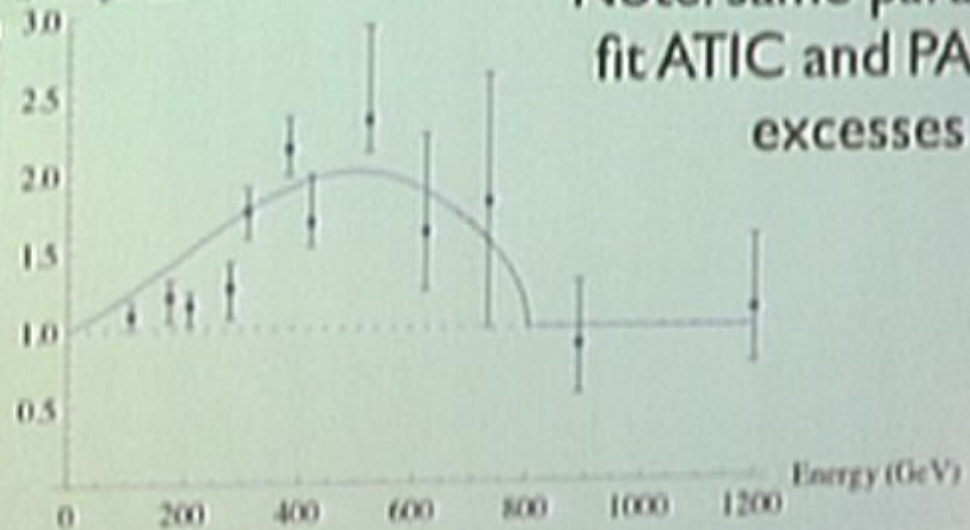
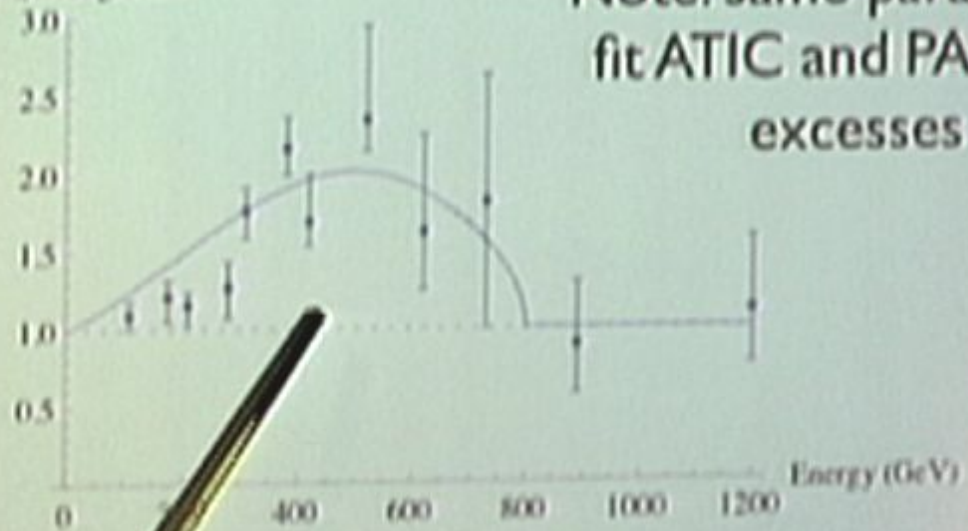


FIG. 3: Ratio of number of electrons to number of background electrons show against the ATIC data for $M = 800$ GeV. The dotted line is the background level, fixed to be 1 in this ratio.

ATIC Feature in Cosmic Electron Spectrum?

$N(e^-)/\text{Background}$

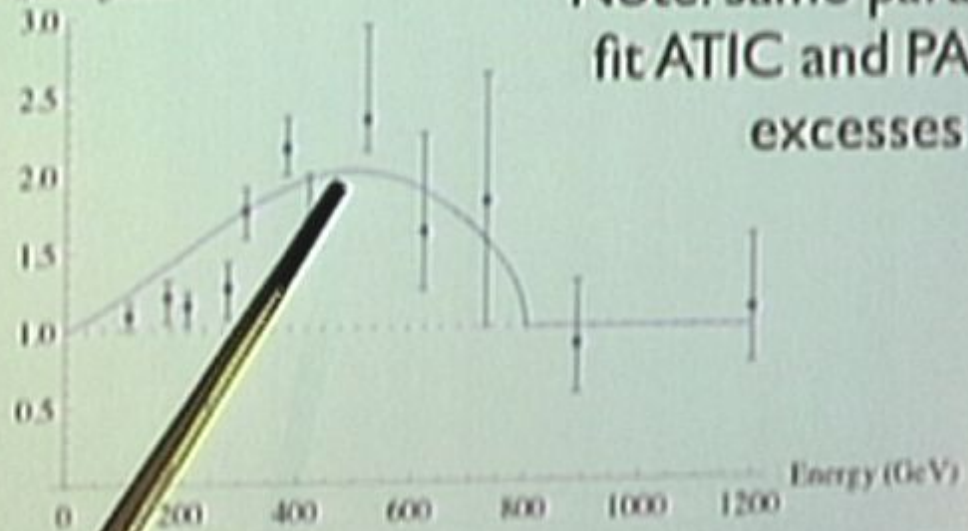


Note: same parameters
fit ATIC and PAMELA
excesses

FIG. 3: Ratio of number of electrons to number of background electrons flow against the ATIC data for $M = 800$ GeV. The dotted line is the background level, fixed to be 1 in this ratio.

ATIC Feature in Cosmic Electron Spectrum?

$N(e^-)/\text{Background}$



Note: same parameters
fit ATIC and PAMELA
excesses

FIG. 3: Ratio of number of electrons to number of background electrons show against the ATIC data for $M = 800$ GeV. The dotted line is the background level, fixed to be 1 in this ratio.

ATIC Feature in Cosmic Electron Spectrum?

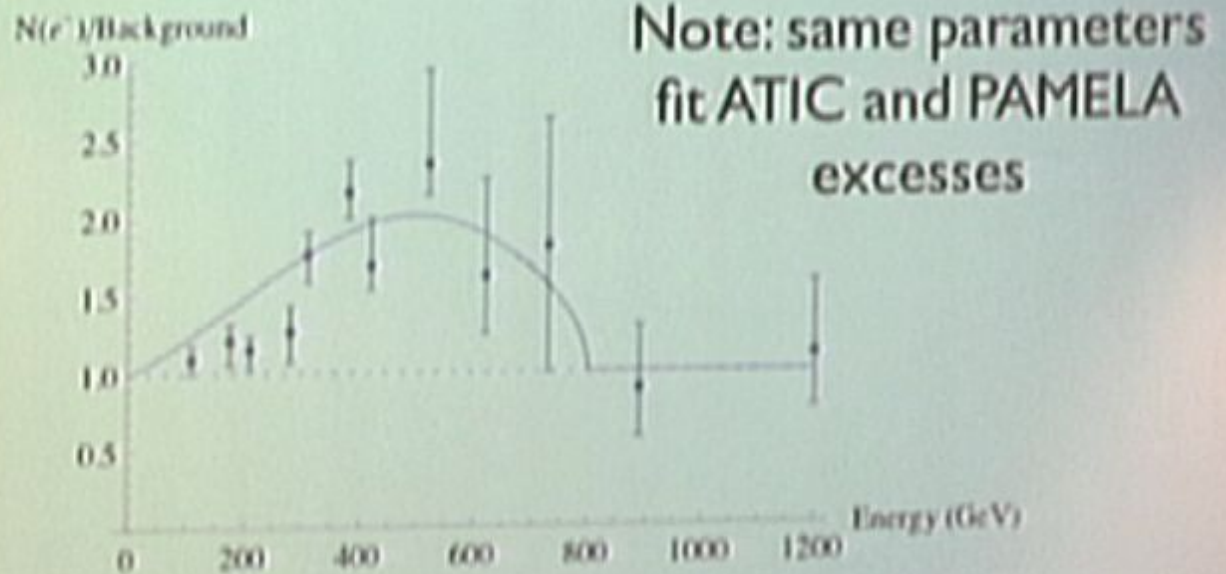


FIG. 3: Ratio of number of electrons to number of background electrons show against the ATIC data for $M = 800$ GeV. The dotted line is the background level, fixed to be 1 in this ratio.

ATIC Feature in Cosmic Electron Spectrum?

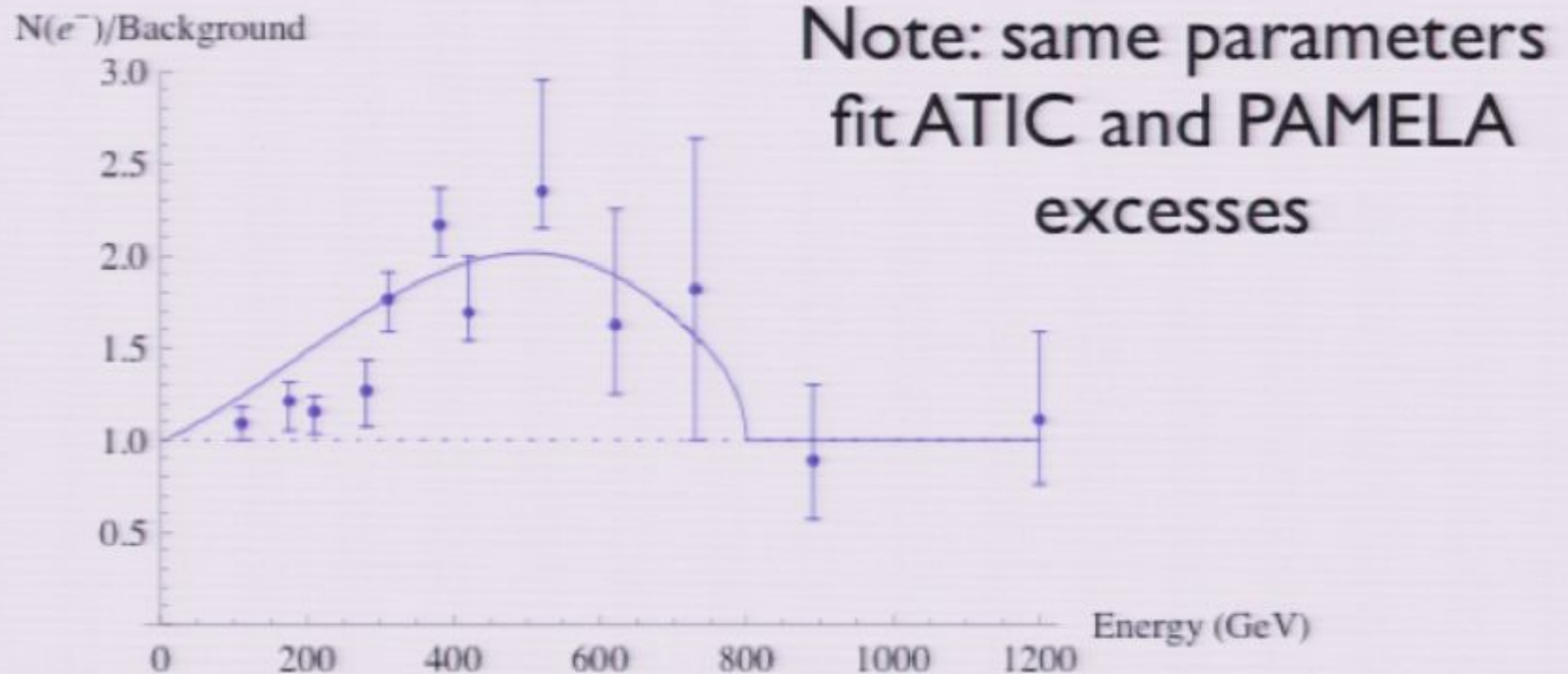
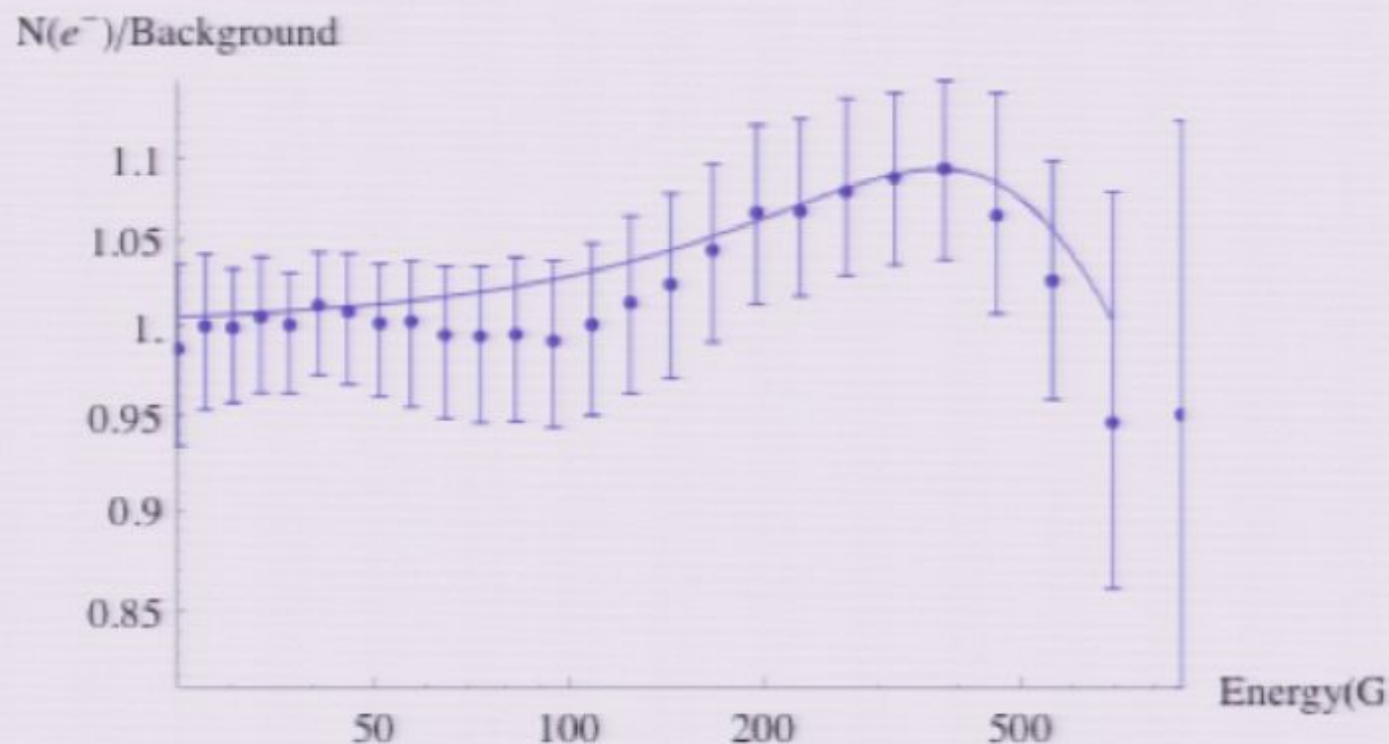


FIG. 3: Ratio of number of electrons to number of background electrons show against the ATIC data for $M = 800$ GeV. The dotted line is the background level, fixed to be 1 in this ratio.

FERMI?

- need to adjust background to explain FERMI + Pamela (or soften spectrum via $\Upsilon \rightarrow \mu^+\mu^-$)



FERMI?

- need to adjust background to explain FERMI + Pamel (or soften spectrum via $\Upsilon \rightarrow \mu^+ \mu^-$)

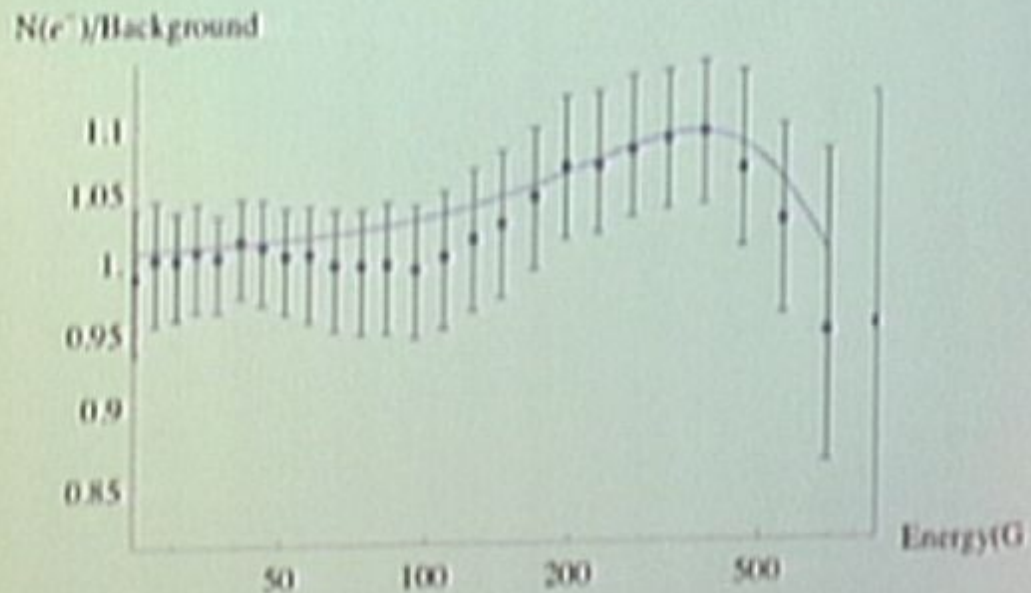


FIG. 6: The ratio of the Fermi signal to background :

FERMI?

- need to adjust background to explain FERMI + Pamel (or soften spectrum via $\Upsilon \rightarrow \mu^+ \mu^-$)

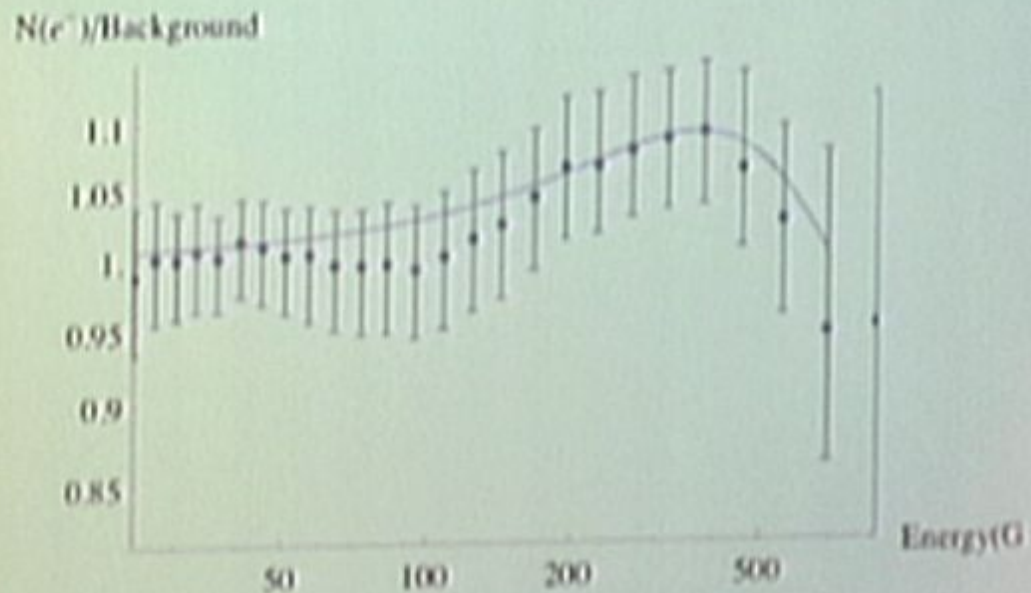


FIG. 6: The ratio of the Fermi signal to background

FERMI?

- need to adjust background to explain FERMI + Pamela (or soften spectrum via $\Upsilon \rightarrow \mu^+ \mu^-$)

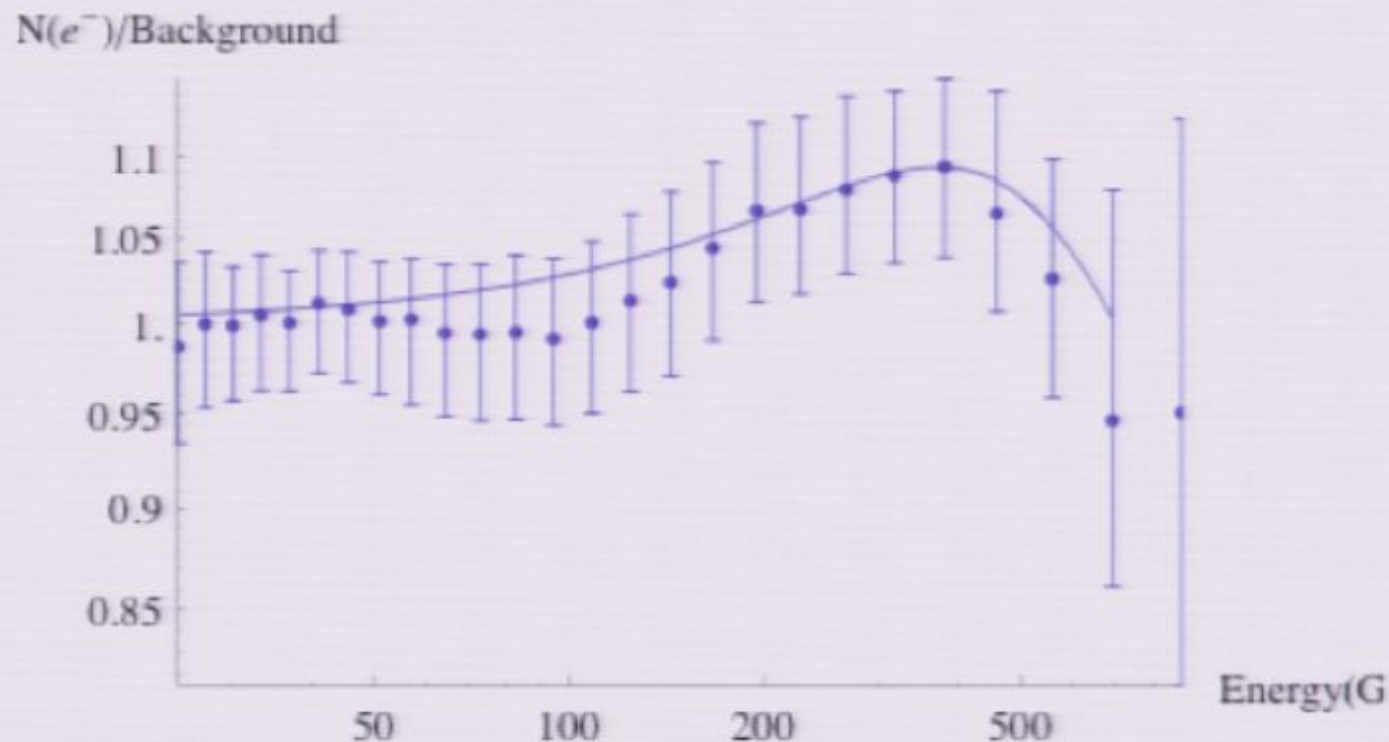


FIG. 6: The ratio of the Fermi signal to background :

Conclusions: current data

- PAMELA, ATIC, FERMI... may have provided first clues to identity of dark matter
- or found new astrophysical source of high energy charged electrons and positrons, e.g. pulsar or pulsars
- if dark matter, must explain large annihilation cross section or huge “boost” factor, lack of antiprotons
- a light “mediator” particle can explain both
- the X, Y, Z_i model is a minimal such model, could be stripped down version of less economical (but more motivated?) hidden sector

Summary

- Era of exploration of dark matter is well underway
- Just as for Electroweak symmetry breaking, consider wide variety of models (not just SUSY/UED WIMP!)
- Especially models with unusual implications for
 - direct detection
 - indirect detection
 - collider production

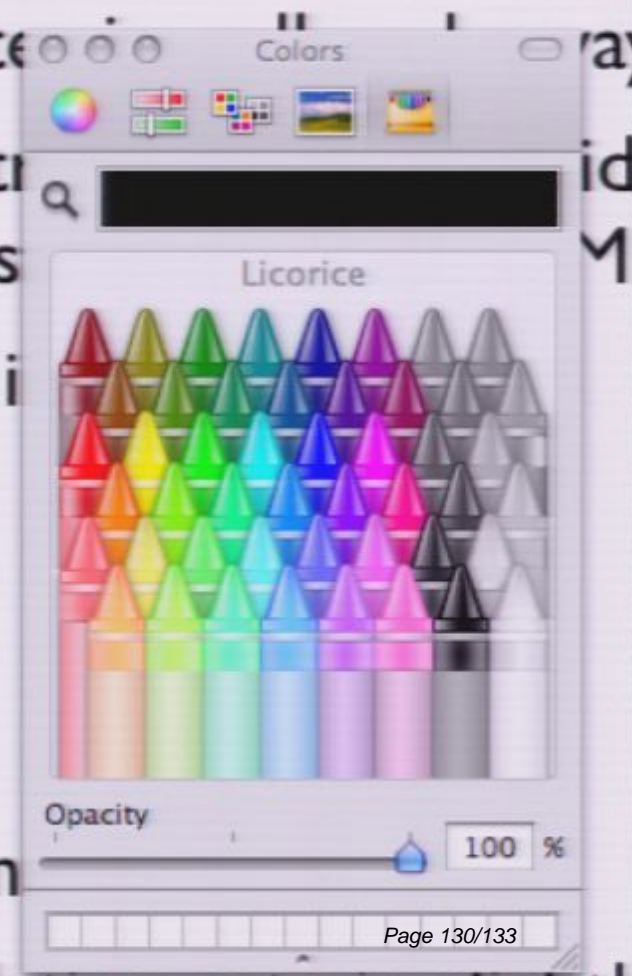
⇒ Non minimal Hidden sector models

- weaker upper bound on annihilation rate in slightly nonthermal

$$\langle \sigma v \rangle < \sim 1.5 \times 10^{-25} \text{ cm}^3/\text{s}$$

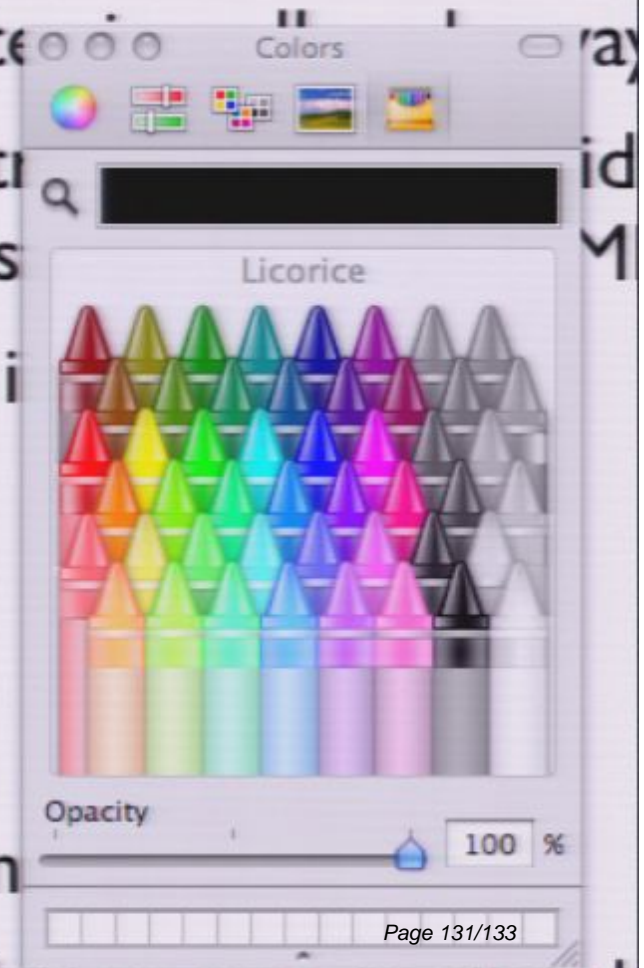
Summary

- Era of exploration of dark matter
- Just as for Electroweak symmetry breaking, a wide variety of models (not just the Standard Model)
- Especially models with unusual interactions
 - direct detection
 - indirect detection
 - collider production
- ⇒ Non minimal Hidden sector models
- weaker upper bound on annihilation rate in slightly



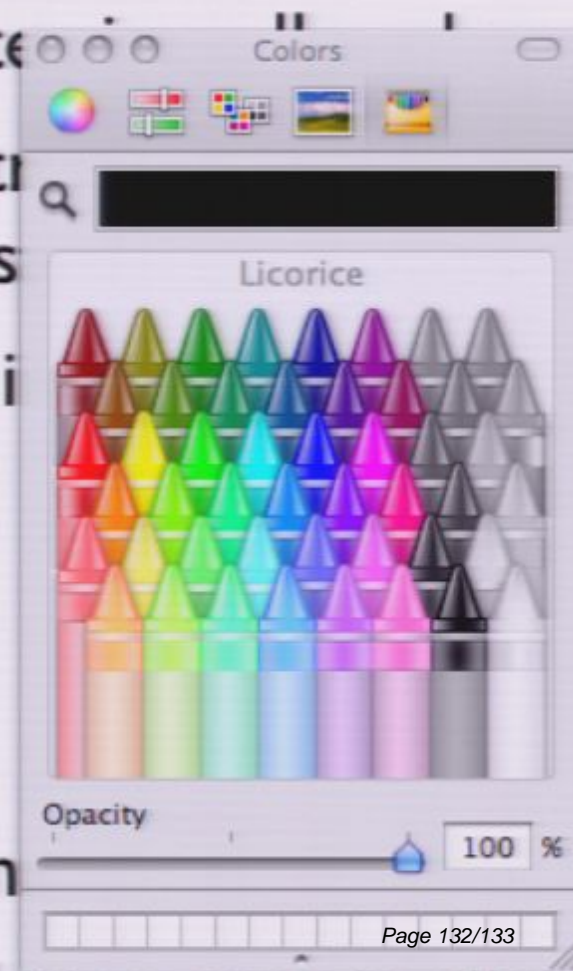
Summary

- Era of exploration of dark matter
 - Just as for Electroweak symmetry breaking, a wide variety of models (not just the Standard Model)
 - Especially models with unusual interactions
 - direct detection
 - indirect detection
 - collider production
- ⇒ Non minimal Hidden sector models
- weaker upper bound on annihilation rate in slightly



Summary

- Era of exploration of dark matter
 - Just as for Electroweak symmetry breaking, a wide variety of models (not just the Standard Model)
 - Especially models with unusual interactions
 - direct detection
 - indirect detection
 - collider production
- ⇒ Non minimal Hidden sector models
- weaker upper bound on annihilation rate in slightly



No Signal

VGA-1